RESEARCH ARTICLE

ESPL WILEY

The role of topography in landform development at an active temperate glacier in Arctic Norway

Clare M. Boston[1] | Benjamin M. P. Chandler[2] | Harold Lovell[1] |
Paul Weber[3] | Bethan J. Davies[4]

[1]School of the Environment, Geography and Geosciences, University of Portsmouth, Portsmouth, UK

[2]School of Geography, University of Nottingham, Nottingham, UK

[3]Quaternary Geology, Geological Survey of Norway, Trondheim, Norway

[4]School of Geography, Politics and Sociology, Newcastle University, Newcastle upon Tyne, UK

Correspondence
Clare M. Boston, School of the Environment, Geography and Geosciences, University of Portsmouth, Portsmouth, UK.
Email: clare.boston@port.ac.uk

Abstract

Topography exerts a strong control on how glaciers respond to changes in climate. Increased understanding of this role is important for both refining model predictions of future rates of glacier recession and for reconstructing climatic change from the glacial geological record. In this paper, we examine the geomorphological and sedimentological evidence in the foreland of Fingerbreen, a temperate outlet of the plateau icefield Østre Svartisen. The aim is to investigate the relationship between processes of landform generation and the changing influence of topography as recession progressed. The Fingerbreen foreland is dominated by bouldery Little Ice Age moraines and extensive areas of striated bedrock. A heavily fluted zone occurs in the central part of the foreland that is cross-cut by annual transverse and sawtooth moraines. Systematic investigations of the structural architecture of moraines at various locations in the foreland provide evidence for a range of moraine-forming processes, which can be linked to the topographic setting (e.g. deposition on a reverse bedrock slope) and drainage conditions. This includes push and bulldozing of proglacial sediments and squeezing of sub-glacial sediments and submarginal freeze-on of sediment slabs. We also identify variations in moraine spacing as a result of topography. This research demonstrates the importance of topography when interpreting moraine records in the context of climate and glacier dynamics.

KEYWORDS
flutes, ice-marginal moraines, Little Ice Age, reverse-bed slope, topographic control

1 | INTRODUCTION

Mountain glaciers are sensitive indicators of climate change (Haeberli et al., 2007), and retreat and thinning of these glaciers has accelerated in recent decades (e.g. Carrivick et al., 2019; Hugonnet et al., 2021; Stokes et al., 2018; Zemp et al., 2015). It is predicted that many mountain glaciers will have disappeared entirely by the end of the 21st Century (Rounce et al., 2023; UNESCO & IUCN, 2022; Zemp et al., 2019). These glaciers currently make a substantial contribution to sea-level rise and, in many mountain regions, make crucial contributions to downstream water supply (Immerzeel et al., 2020). They also provide ecosystem services and are important to many economies for tourism (Antoniazza & Lane, 2021; Beniston et al., 2018).

During their recession, mountain glaciers leave a wealth of geomorphological and sedimentological data that document their dynamics and response to climate change (e.g. Bennett, 2001; Evans, 2003; Evans et al., 2019; Le Heron et al., 2022; Weber et al., 2019). These terrestrial archives can record decadal to sub-annual changes in glacier- and climate-related dynamics (e.g. Chandler et al., 2016; Chandler, Evans, et al., 2020; Lukas, 2012; Reinardy et al., 2013). Ice-marginal moraines are particularly important archives because they mark the position of a former glacier margin. This has allowed moraines to be used to reconstruct the extent and age of palaeoglaciers and to estimate past climate (e.g. Boston et al., 2015). However, many studies have demonstrated the role that topography plays in moderating the response of glaciers to climate change (e.g. Barr & Lovell, 2014; Boston & Lukas, 2019;

Davies et al., 2022; Magrani et al., 2021; Oerlemans, 2012; Pedersen & Egholm, 2013), which may have implications for using moraines to reconstruct palaeoglaciers (Rowan et al., 2022). Processes of glacial landform development are thus affected by the interplay of glaciological, climatic and topographic factors. Documenting this geomorphological imprint, and investigating the associated sub-glacial and ice-marginal processes responsible, offers a detailed insight into changes in individual glacier dynamics over time (e.g. Chandler et al., 2016; Chandler, Evans, et al., 2020; Chandler, Lukas, & Boston, 2020; Evans et al., 2019; Hiemstra et al., 2022; Lukas, 2012; Weber et al., 2019), which can help to understand the role of topography in glacial landform generation.

At temperate non-surging glaciers, ice-marginal moraines can be constructed by seasonal cycles of submarginal squeezing and bulldozing, where water-saturated sub-glacial sediment is squeezed from beneath the margin (in the summer) and subsequently bulldozed during minor winter re-advances (e.g. Chandler et al., 2016; Chandler, Chandler, et al., 2020; Price, 1970; Sharp, 1984). Bulldozing of previously deposited glaciogenic sediments can also occur (e.g. Chandler et al., 2016; Chandler, Chandler, et al., 2020; Lukas, 2012; Wyshnytzky et al., 2020). Moraines can also form as ice-contact fans (e.g. Krzyszkowski & Zieliński, 2002; Lukas, 2005, 2012), where sediment is delivered from the ice surface to the ice margin through debris flow and fluvial processes, rather than via a sub-glacial mechanism.

Some temperate glaciers are known to have cold-based glacier margins or marginal zones where the margin is sufficiently thin enough to allow the winter freezing front to penetrate beneath the glacier (e.g. Reinardy et al., 2019). This thermal regime can provide favourable conditions for the freeze-on of submarginal sediment slabs/layers to the glacier undersole during winter. Subsequent transport and meltout of these sediment slabs can lead to moraine formation (Evans & Hiemstra, 2005; Krüger, 1994, 1995, 1996; Matthews et al., 1995; Reinardy et al., 2013). The process of slab freeze-on may be further facilitated by the presence of saturated sediments around and beneath the glacier margin prior to freezing (Chandler et al., 2016).

Topography not only controls larger-scale patterns of moraine spacing (e.g. Barr & Lovell, 2014) but it also influences the shape of the ice margin (Evans et al., 2016) and foreland drainage conditions (Marren & Toomath, 2014), which in turn affects moraine-forming processes. For example, at active temperate glaciers in Iceland, topographically controlled changes in (a) glacier snout morphology and structural architecture and (b) submarginal to ice-marginal drainage conditions have been argued to be key controls on processes of moraine formation (e.g. Chandler et al., 2016; Chandler, Chandler, et al., 2020; Chandler, Evans, et al., 2020; Evans et al., 2016, 2017, 2018, 2019). Specifically, glacier thinning and snout recession into overdeepenings have resulted in heavily crevassed glacier margins and a switch to constrained, poorly drained submarginal and ice-marginal conditions. Such conditions are favourable for ice-marginal squeezing of sub-glacial tills through radial marginal crevasses (pecten), resulting in the formation of sawtooth and hairpin-shaped moraines during the past ~30 years (e.g. Chandler, Chandler, et al., 2020; Chandler, Evans, et al., 2020; Evans et al., 2016; Everest et al., 2017; Jónsson et al., 2016).

In this paper, we focus on the Norwegian glacier Fingerbreen, which is an outlet of the plateau icefield Østre Svartisen (Figure 1). Norwegian glaciers lost 10% of their area between the 1960s and 2010s (Andreassen et al., 2020). Many of the icefields are dominated by low-slope accumulation areas and so are considered particularly vulnerable to the current warming trends (Giesen & Oerlemans, 2010; Stokes et al., 2018; Zemp et al., 2019). Indeed, Østre Svartisen lost the largest area (55 km^2) between the 1999–2006 and 2018–2019 Norwegian glacier inventories (Andreassen et al., 2022). Few studies have investigated the relationship between changes in glacier dynamics, topography and processes of ice-marginal landform generation at Norwegian glacier margins, particularly since the 2000s when glacier recession rates have accelerated (e.g. Hiemstra et al., 2015; Weber et al., 2019; Winkler & Matthews, 2010). The aim of this research is therefore to investigate processes of landform generation at Fingerbreen and examine how topography influences the glacier's response to changing climatic conditions.

2 | STUDY AREA AND PREVIOUS RESEARCH

Fingerbreen is a major outlet glacier of the Østre Svartisen plateau icefield, which is located just inside the Arctic Circle (66°N) in Norway (Figure 1). Glaciers in the region are considered temperate (Paul & Andreassen, 2009). Fingerbreen has a large, low-slope plateau accumulation area with an ice-surface altitude of over 1000 m, from which the glacier flows down through a narrow valley to around 450 m asl. In 1996, Fingerbreen was flowing at a maximum horizontal velocity of 0.38 m/day in a narrow zone close to the plateau edge, reducing to 0.05–0.1 m/day near the margin (Sharov, 2003). The area is underlain by Cambrian and Silurian mica schists and intrusive igneous (mainly granitic) rocks (Gurney & White, 2005; Holtedahl, 1960).

Fingerbreen reached its 'Little Ice Age' (LIA) maximum position around 1747 AD (Winkler, 2003), similar to ice masses in southern Norway (e.g. Hardangerjokulen: Weber et al., 2019; Jostedalsbreen: Carrivick et al., 2022). In 1882–1890, Fingerbreen was within 200 m of the LIA moraine according to Rabot (1898) and Rekstad (1893) (see Theakstone, 2010). Since then, the glacier has retreated ~2.5 km from its LIA position (Figure 1b). Field surveys and photogrammetry undertaken during the 1960s and 1970s found that the ice-marginal zone thinned by 8–10 m between 1945 and 1981 (see Knudsen & Theakstone, 1984). Between 1968 and 1999, Fingerbreen lost 3%–8% of its area (Paul & Andreassen, 2009). Østre Svartisen as a whole lost ~23% of its area between 1899 and 2000 (Weber et al., 2020).

3 | METHODS

Geomorphological mapping of the glacier foreland was completed using high-resolution (25 cm) colour digital aerial photographs from 2014 and 2019 (Table 1) and 1:10 000-scale field mapping of the area north of the main meltwater channel, undertaken in August 2016. Using a standard approach (e.g. Chandler et al., 2018), key erosional and depositional glacial landforms (e.g. moraines, meltwater channels, flutings, ice-smoothed bedrock) were mapped digitally in Esri ArcGIS before field verification. Field data were then combined with further remote mapping to produce the final geomorphological map. In the field, a handheld GPS (accuracy ~3 m) was used to provide positional accuracy of smaller features, and the orientations of 25 striae were measured at 41 locations using a compass.
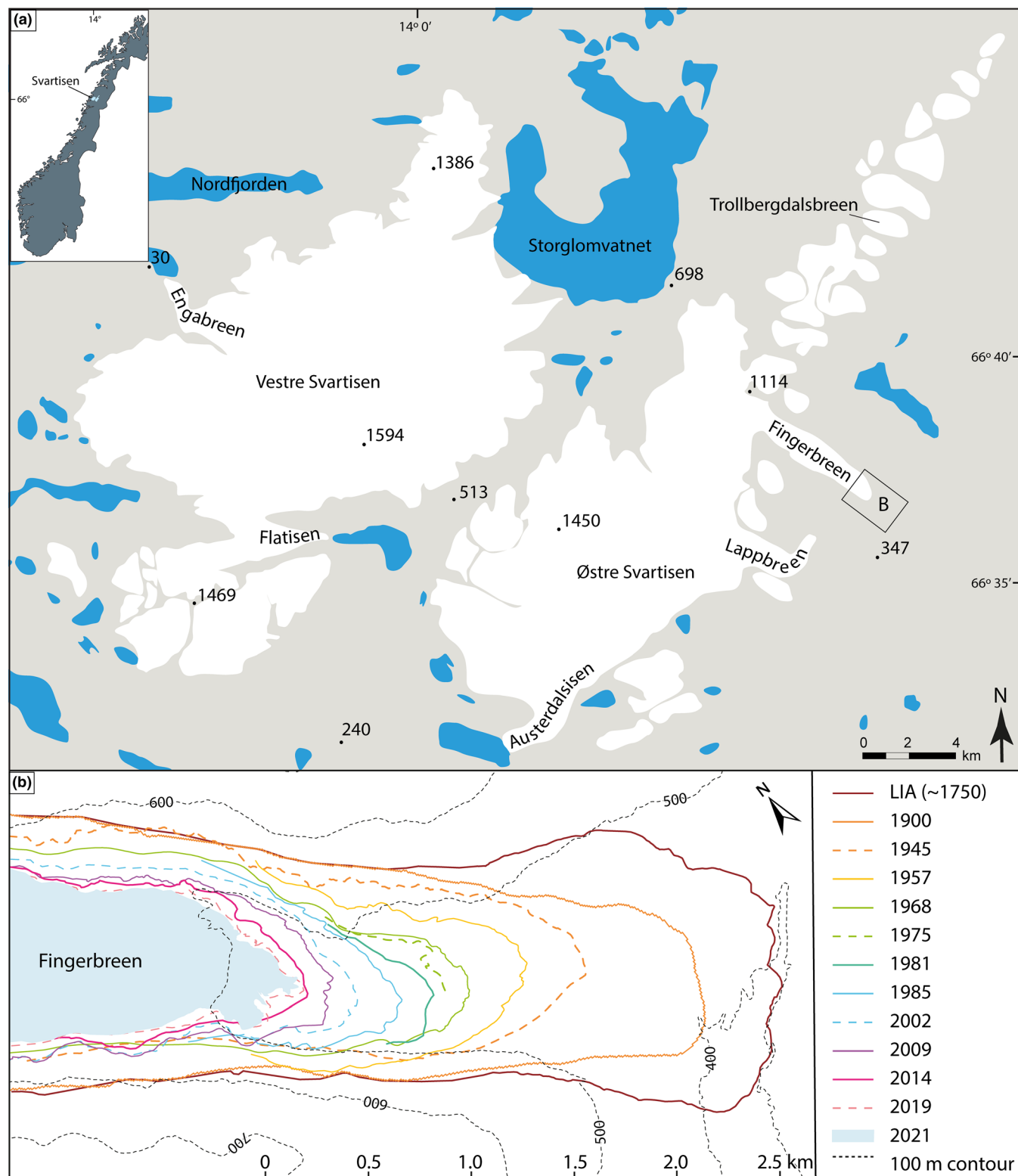
FIGURE 1 (a) Study area map showing the location of the study site at Fingerbreen, including spot heights in metres above sea level (asl). (b) Previous known positions of Fingerbreen. Sources for these ice margin positions are listed in Table 1.

The LIA maximum was identified by the outermost moraines, a reduction in vegetation or a change from weathered to smoothed bedrock. Former ice marginal positions were derived from panchromatic and colour aerial photographs and previously published limits (Knudsen & Theakstone, 1984) (Table 1 and Figure 1b). The panchromatic aerial photographs were georegistered to the colour orthophotos using prominent and stable landscape features visible on both datasets as control points. A spline transformation was used with a large number of control points (>100) due to the high level of radial distortion caused by the large altitudinal range within any one photograph.

To examine processes of landform generation, small sections were excavated within flutes and moraines. Section logging involved recording overall section architecture, particle size, degree of sorting

TABLE 1 Sources of data of former ice margin positions at Fingerbreen.

Data type	Year	Source
Geomorphological observations and lichenometry measurements	1750	Lichenometry: Winkler (2003)
Digitised gradteigskart (map sheet K15 Dunderlandsdalen)	1900 (surveyed 1894–1896)	Weber et al. (2020)
Panchromatic aerial photograph	1945	Royal Air Force
Panchromatic aerial photograph	1957, 1968, 1985, 2002	Widerøe
Photogrammetric surveys	1975, 1981	Knudsen and Theakstone (1984)
Colour digital aerial photograph	2009, 2014, 2019	Norgeibilder (https://norgeibilder.no/)
Esri ArcGIS World Imagery	2021	Maxar
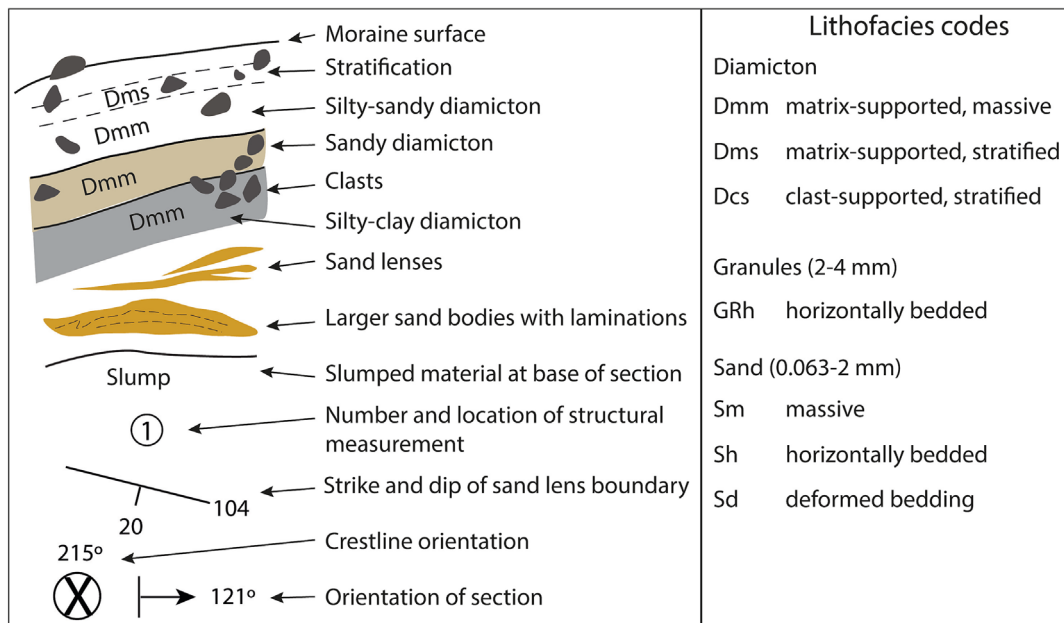
FIGURE 2 Legend for sedimentary logs (after Lukas, 2012).

and bedding plane dip and strike, as described in Evans & Benn (2021) (Figure 2). Samples for clast shape and roundness analysis were also collected at each section and compared with supraglacial and fluvial control samples, using the approach described by Lukas et al. (2013). Each sample contained 50 mica schist clasts, and the data were plotted and analysed in Triplot (Graham & Midgley, 2000).

4 | RESULTS

4.1 | Geomorphology

The glacial geomorphology of the foreland is presented in Figure 3a. We divide the foreland into three zones based on different topographic characteristics and landform-sediment assemblages (Figure 3b). Zone 1 comprises the LIA limit, the central foreland up to 1.1 km upvalley of the LIA and the lateral margins up to 1.9 km upvalley of the LIA limit. The area is characterised by large bouldery moraines close to the LIA limit, which become smaller upvalley, interspersed by areas of striated bedrock. Zone 2 comprises a flat, heavily fluted area in the central part of the foreland, 1.1–1.9 km upvalley

from the LIA limit, which is cross-cut by transverse (straight) and sawtooth (zig-zag) frontal moraines. Zone 3 features latero-frontal moraines deposited on top of a bedrock high and its reverse (ice-proximal) slope and includes the present-day ice margin. This zone begins around 1.9 km upvalley from the LIA limit.

4.1.1 | Zone 1 landform-sediment assemblages

The LIA limit is clearly delimited by an outer perimeter of large bouldery moraine ridges (Figures 3 and 4a,b). Inside the LIA limit, there is a notable reduction in vegetation, smaller lichen diameters (typically <100 mm) and glacially smoothed unweathered bedrock. The LIA lateral moraine on the southwestern valley side forms a continuous ridge, which breaks into a chain of shorter ridges across the central part of the valley floor. The outermost moraines on the southwestern valley side are some of the largest in the foreland (>5 m in height) and are composed of large boulders (particularly at the lateral margins) with a sediment matrix. In comparison to these well-defined moraines, the moraines on the northeastern side are constructed solely of boulders, sometimes comprising a single boulder line (Figure 4a).
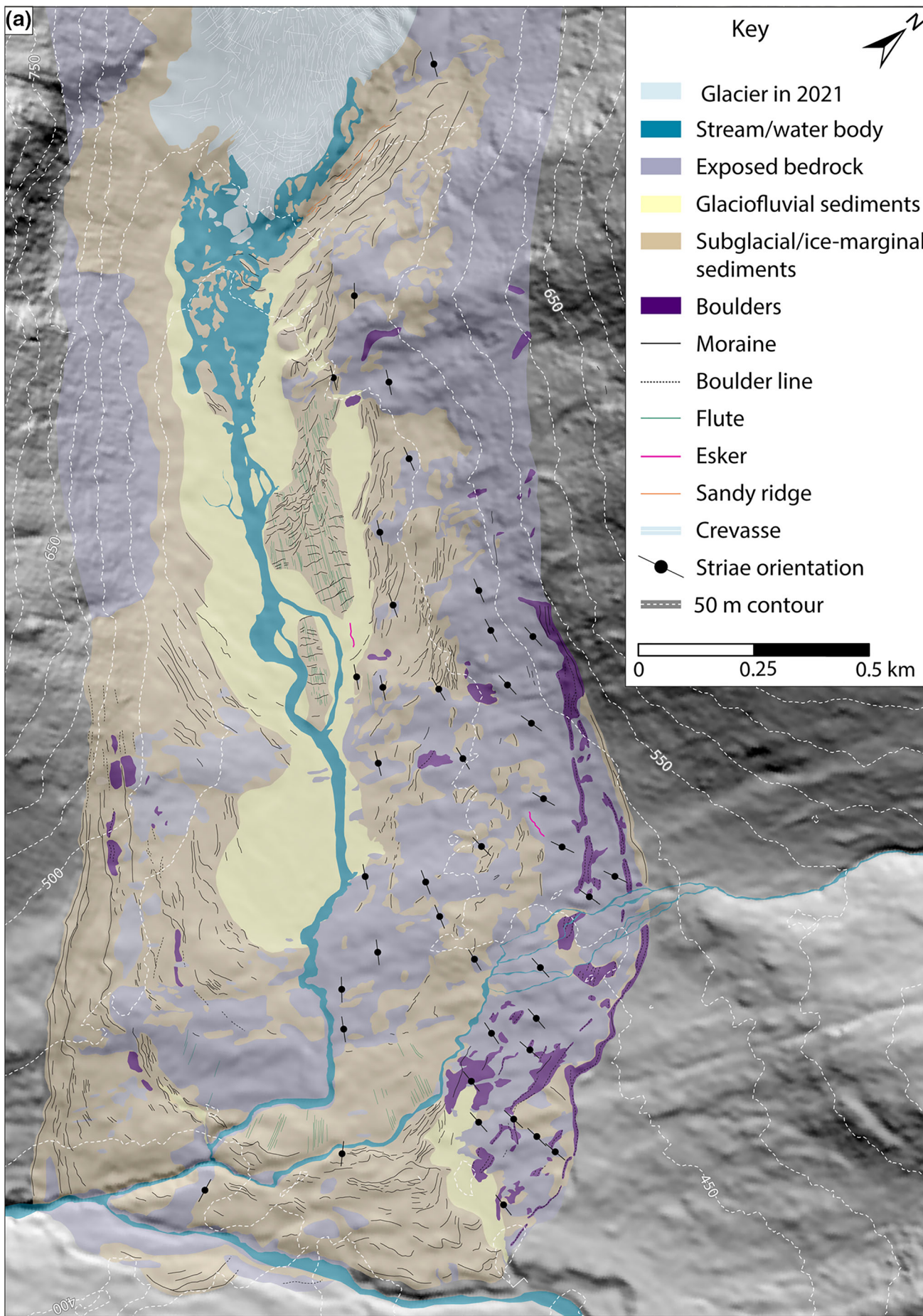
FIGURE 3 (a) Glacial geomorphological and surficial geological map of the Fingerbreen foreland. (b) Subdivision of the Fingerbreen foreland into three zones based on topographic and geomorphological characteristics. Inset box is the location of Figure 3c. (c) Location of section logs discussed in the text.
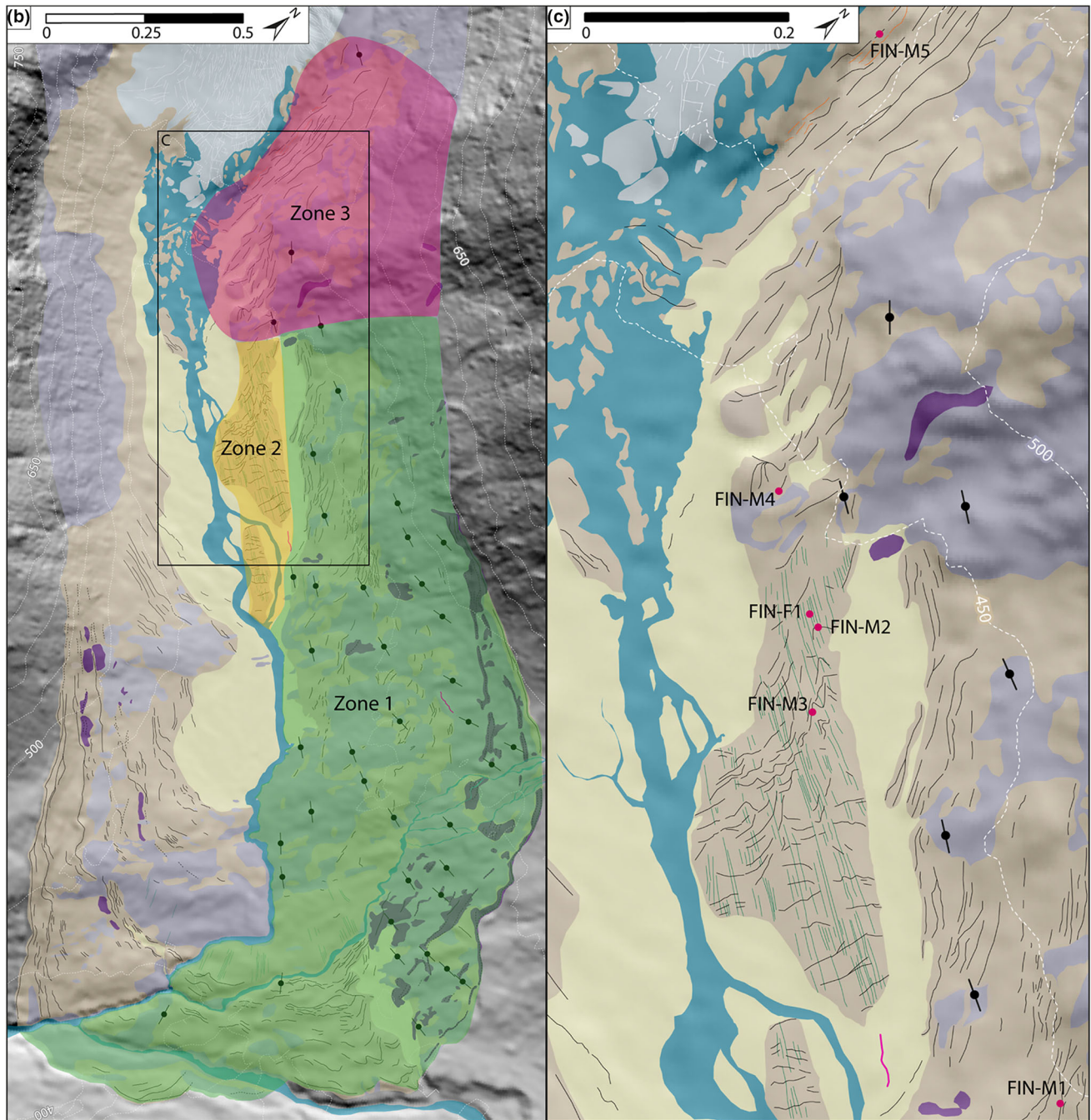
FIGURE 3 (Continued)

Inside the LIA limit, moraines occur in clusters of around five closely spaced ridge chains, with gaps of 50–250 m between the clusters. These inset moraines display similarly distinct differences in composition between the northeastern (boulders only; Figure 4a) and southwestern valley sides (matrix-supported boulders). This within-valley asymmetry is apparent throughout the lower part of the catchment, with an increased number of more prominent moraines on the southwestern valley side.

Bedrock is dominant on the northeastern valley side from ∼400 m upvalley of the LIA limit, forming an undulating surface with minor reverse-bed slopes. Glacially derived debris is scattered on much of this bedrock forming a thin veneer, while small moraine-ridge fragments tend to be located on outcrop crests. Conversely, clusters of larger

moraines occur within large-scale hollows in the bedrock. Two eskers occur, several hundred metres apart, close to these moraine clusters. Exposed bedrock is heavily striated, with mean striae orientations of 241–061° at former lateral margins and 334–154° closer to the former central flowline (Figure 3a). Close to the latero-frontal LIA limit and central flow line, there is little variation (10° to 15°) in striae orientation. Striae near the lateral LIA limit show a wider spread of orientations or two dominant orientations. Directly cross-cutting striae were only found at one location. In contrast to the bedrock-dominated northeastern valley side, from ∼700 m upvalley of the LIA limit, the southwestern side is predominantly covered by glaciofluvial sediments and former meltwater channels close to the main meltwater channel (Figure 4b), and by bouldery moraines/debris on the steeper slopes.
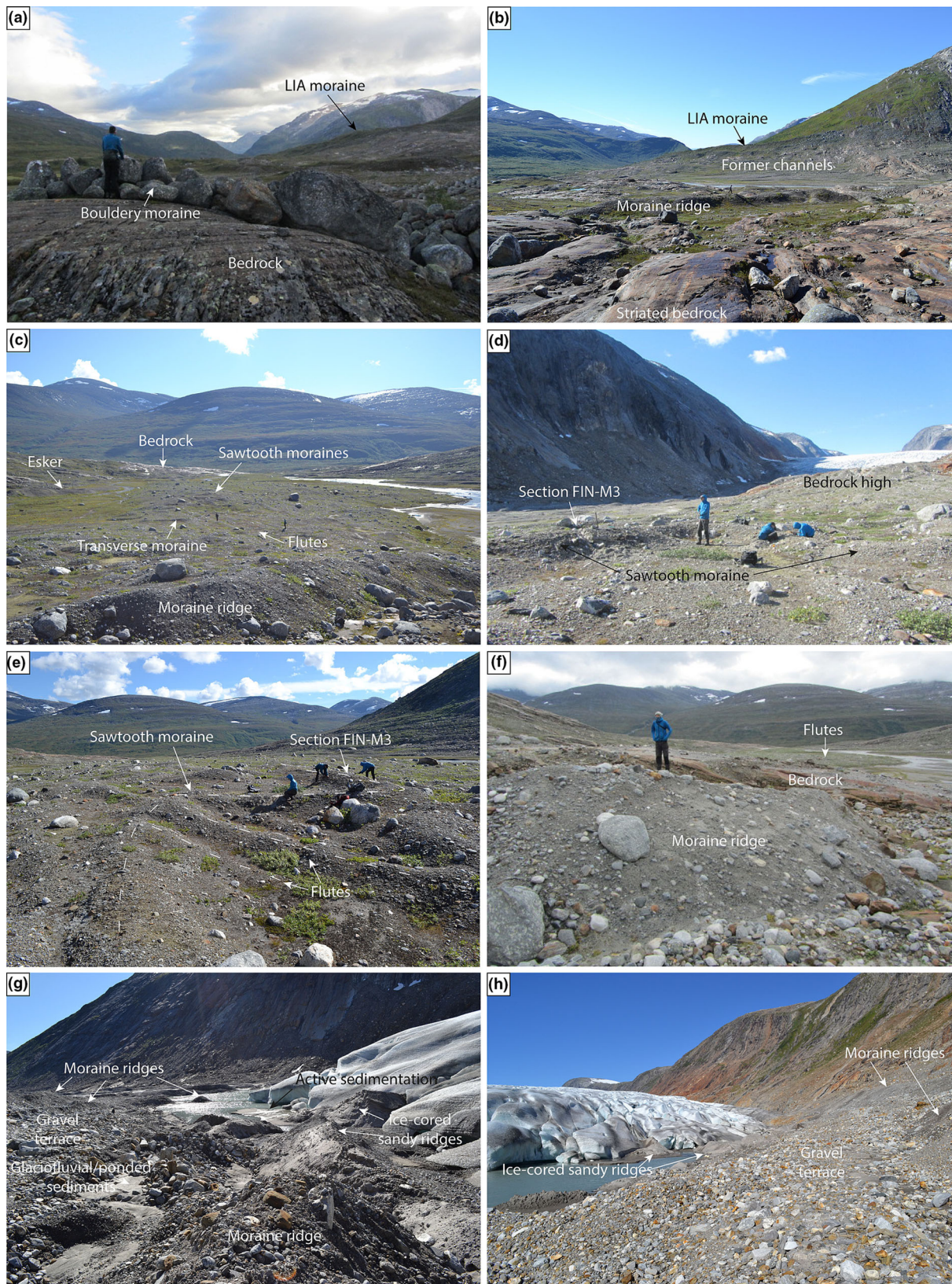
FIGURE 4 Photographs of the Fingerbreen foreland. (a) Bouldery moraine with no sediment matrix on the northern valley side close to the LIA limit, view towards the southwest. (b) View southwest across the foreland, showing LIA maximum moraines on the southwestern valley side and the area within Zone 1. (c) View downvalley of Zone 2 showing transverse and sawtooth moraines and flutes. (d) View upvalley of a sawtooth moraine within Zone 2, with the bedrock high in the background. (e) Close-up of a sawtooth moraine and flutes, showing how the flutes onlap the moraine on the up-ice side. (f) View downvalley of a moraine on top of the bedrock high in Zone 3. (g) View south along the 2016 ice margin, with moraines and ice-cored sandy ridges within Zone 3. (h) View north along the reverse slope of the bedrock high in Zone 3 and the 2016 ice margin.

4.1.2 | Zone 2 landform-sediment assemblages

This zone constitutes a raised area in the centre of the foreland that has been undisturbed by glaciofluvial activity (Figures 3 and 4c–e). It is bounded to the southwest by the main meltwater channel and to the northeast by a former channel. The area is dominated by flutes that are cross-cut (overlain) by transverse and sawtooth moraines. These moraines and flutes are very low profile with amplitudes of ~0.4 m. In 1957, the ice margin was located at the southeastern (downvalley) edge of Zone 2 (Figure 5a). By 1968, Fingerbreen had retreated approximately halfway across this zone (Figure 5b). The whole zone had been exposed by 1985 (Figure 5c). Transverse moraines occur throughout Zone 2, although they are mostly concentrated in the downvalley half. In the upvalley half, sawtooth moraines are more prevalent (Figure 3c).

The flutes have an average length of 26 m, mean orientation of 112° and range in width between 1 and 4 m. The average width of a subsample of 30 flutes is 1.9 m and remains constant in both the upvalley and downvalley parts of the zone. In the upvalley half, the cross-cutting sawtooth moraines often appear to disturb the flutes.
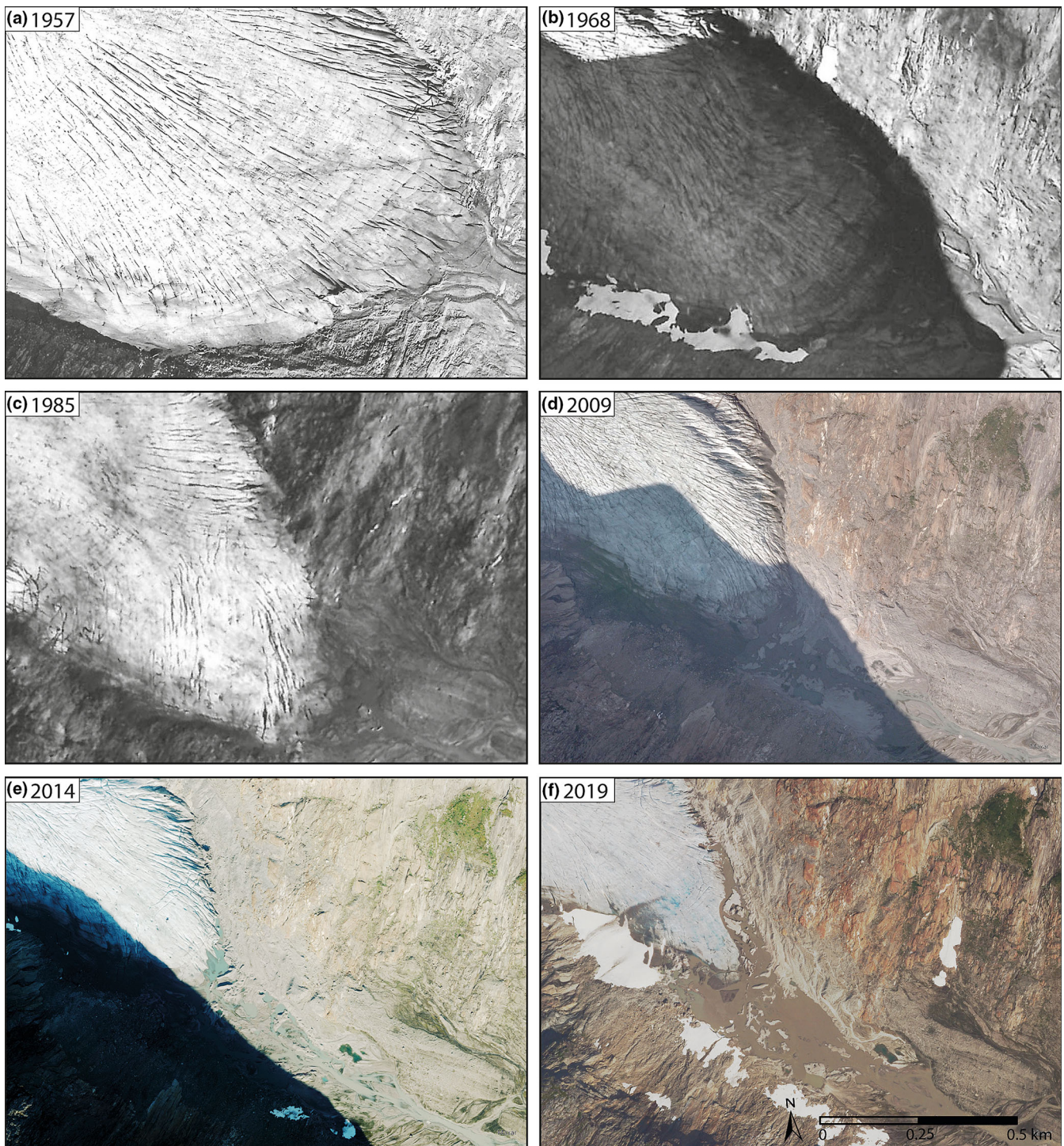
FIGURE 5 Aerial photographs of the Fingerbreen margin: (a) 1957, (b) 1968, (c) 1985, (d) 2009, (e) 2014, (f) 2019. *Source*: Widerøe (owner: NVE) and Norgeibilder (see Table 1 for details).

Examples of this include flutes that overlay the moraines on the ice-proximal side (Figure 4e) and/or disappear/change direction on the distal side. Conversely, the flutes generally remain undisturbed beneath the transverse moraines.

4.1.3 | Zone 3 landform-sediment assemblages

Zone 3 encompasses the most recently deglaciated area, extending from a large bedrock high (∼10–15 m above the valley floor) on the northeastern valley side to the present ice margin (Figures 3b and 4d). In this zone, a series of latero-frontal moraines occur on the top of the bedrock high and down its reverse (ice-proximal) slope. Moraines on top of the bedrock high (Figure 4f) formed sometime between 1985 and 2002 and thereafter were deposited on the reverse slope (Figure 4h). Moraines on the reverse slope are composed of a very loose, boulder-rich, clast-supported sandy diamicton and are interspersed with glaciofluvial cobble terraces. At the southwestern glacier margin, the area consists of steep bedrock with some glacial debris, but no moraines, at the base. The glacier is currently receding into what appears to be an overdeepening, and a lake has formed in front of the central portion of the glacier (Figures 3 and 4g,h). This small lake has existed since at least 2002 and expanded significantly between 2014 and 2019 (Figure 5). Consequently, moraine development has become increasingly restricted around the glacier margin.

In 2016, the area immediately in front of the northeastern ice margin consisted of small 0.5 m high moraines. These were interspersed by ridges of sorted sediments (mainly sands), with heights of 0.5–3 m (Figure 4g). The larger of these sandy ridges were ice-cored. In general, the sand ridges were orientated perpendicular to ice flow and at a similar orientation to the moraines. However, in places, the sorted sediment ridges curved around nearly 90° and appeared to emanate from longitudinal crevasses, mimicking the shape of the glacier margin. Several small ice caves in the margin provided a view of the glacier bed and revealed that the visible clean ice is overlain on top of a 1–2 m thick layer of debris-covered ice. Exposures by the lake also revealed a significant quantity of buried glacier ice in the proglacial area.

4.2 | Sedimentology

Below, we present a selection of six sections that we consider a representative subsample of the lithofacies (LFs) found within a large number of moraines and flutes examined across the Fingerbreen foreland. The age of these landforms was estimated using aerial photographs and previously published limits (Figure 1b).

4.2.1 | Lateral moraine, Zone 1

Description: Section FIN-M1 (Figure 6) was excavated within a lateral moraine on the northeastern valley side that formed between 1945 and 1957. The moraine is 1.5–2 m high and >1.5 m wide with a rounded crestline and surface composition of cobble-sized clasts to small boulders. The moraine crestline is orientated at 132–312°, and the section orientation was 040–220°. The moraine is predominantly composed of a loose diamiction, with a coarse sand to fine gravel matrix, which is predominantly massive and matrix supported, but shows some stratification in places and is clast supported towards the top (LF 1). A number of fine sand bodies and lenses containing deformed wavy bedding occur in the lower part of the section. The lenses dip towards the ice-proximal side and structural measurements at the upper boundary of one sand lens had dips of 19° and 24° and strikes of 133° and 140°, respectively (Figure 6). A larger body of fine sand in the centre of the section displayed a dip of 72° and strike of 301°, that is, eastwards towards the valley side. Clast shape and roundness analysis shows that clasts within the moraine are blocky (C_{40}:18) and subangular to rounded (RA:0; RWR:18) (Figure 7).

Interpretation: The loose, sandy to fine gravel matrix of LF 1 and subangular to rounded clasts that collectively plot close to the glaciofluvial control samples (Figure 7) suggests that the moraine was formed from pre-existing glaciofluvial sediments (e.g. Lukas, 2012; Wyshnytzky et al., 2020). The sand body and lenses within the moraine are therefore interpreted as glaciofluvial sediments, originally deposited either as low energy streams or inflows into localised ponds close to the glacier margin, that have subsequently been displaced and incorporated into the moraine (e.g. Chandler et al., 2016;
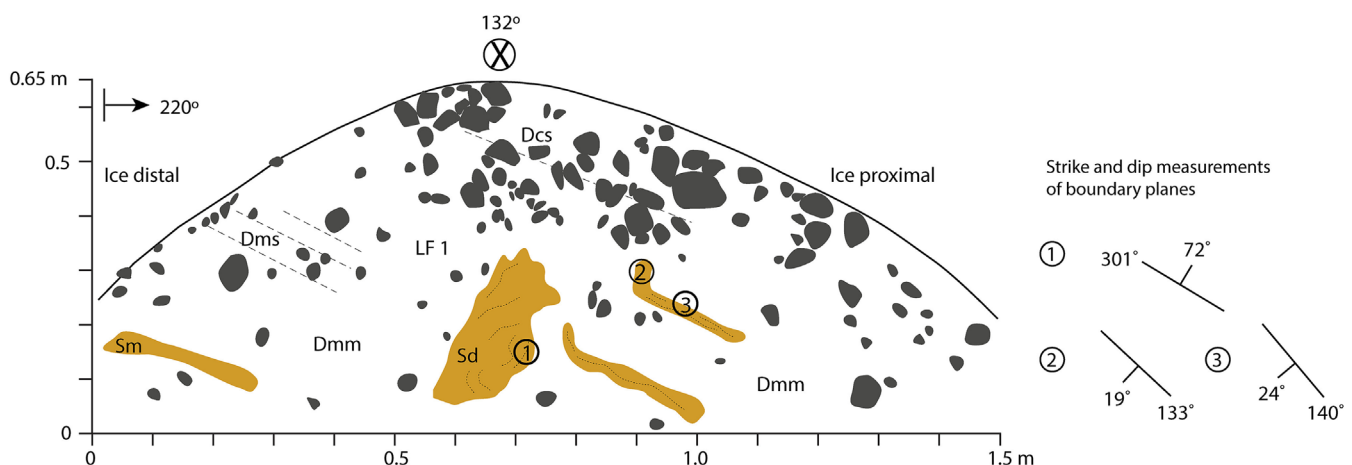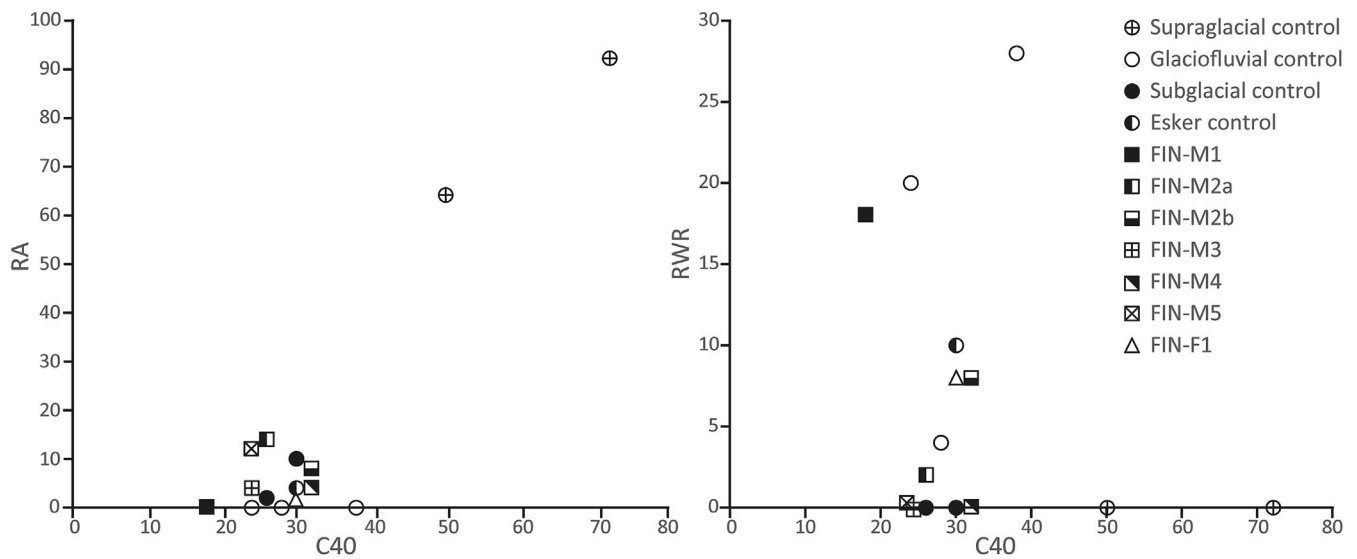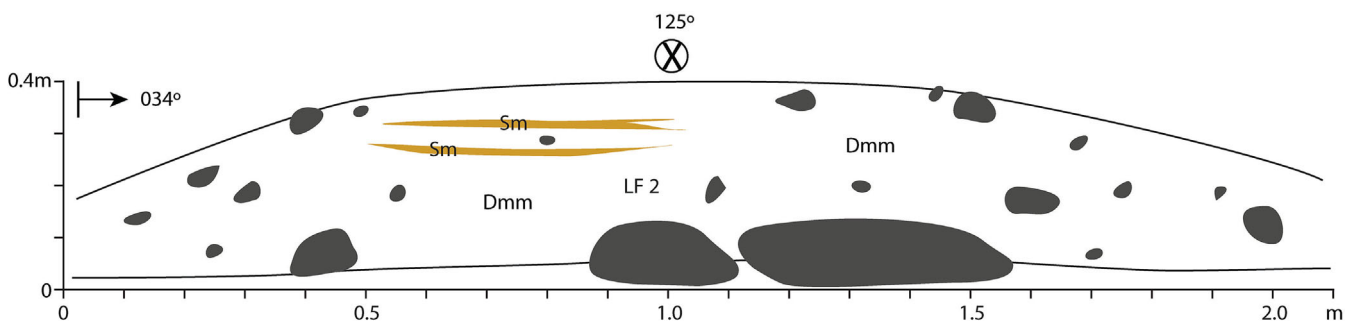

FIGURE 6 Log of section FIN-M1.

FIGURE 7 RA and RWR covariance plots for clast shape and roundness analysis on mica schist for supraglacial, sub-glacial, glaciofluvial and esker control samples and samples taken from moraine and flute sections.

FIGURE 8 Log of section FIN-F1.

Chandler, Chandler, et al., 2020; Lukas, 2012; Reinardy et al., 2013; Wyshnytzky et al., 2020) (e.g. Figure 4g).

The near 180° variation in the dip direction of the sand lenses is indicative of folding, and we suggest that the sand body and lenses in the central part of the section represent the apex of a large fold, indicative of compressional deformation (McCarroll & Rijsdijk, 2003). Smaller-scale soft-sediment deformation occurred simultaneously within the sand lenses. We suggest that the moraine formed as a result of proglacial deformation (pushing) of pre-existing glaciofluvial sediments at the ice margin during ice advance (Chandler, Chandler, et al., 2020; Lukas, 2012; Winkler & Matthews, 2010).

4.2.2 | Flute, Zone 2

Description: Section FIN-F1 (Figure 8) was cut into a >2.1 m wide, 25 m long, flute, which had a height of 0.4 m and crestline orientation of 125–305°. The flute is composed of a massive silty-sandy diamicton, with thin horizontally bedded lenses and wisps of sand (LF 2). Clast size ranges from granules to boulders, some of which are striated. The clasts are relatively blocky (C_{40}:30) and predominantly subangular to subrounded (RA:2; RWR:8) (Figure 7).

Interpretation: Based on the occurrence of striated clasts, the fine-grained sediment matrix and massive structure of LF 2, we interpret it as a sub-glacial traction till (sensu Evans et al., 2006). A subglacial origin for the diamicton is also broadly supported by the clast shape and roundness data, although the sample also plots closely with the esker control sample in Figure 7. We suggest that the small sand lenses and stringers within the diamicton are sliding bed facies resulting from fluctuating pore water pressures (Ives & Iverson, 2019), possibly combined with sediment washing during ice-bed decoupling events (Larsen et al., 2006) and subsequent shearing within the deforming layer (Kessler et al., 2012).

4.2.3 | Transverse moraine, Zone 2

Description: Section FIN-M2 (Figure 9) was created across a 2.6 m wide transverse moraine, with a height of 0.4 m and orientation of 215–395°, which is perpendicular to the former ice-flow direction. The section is composed of two diamictons, separated by a convoluted and folded boundary. The lower diamicton is 0.2 m thick, massive and has a dark silty-sandy matrix, similar to LF 2 in FIN-F1, although contains more clasts. The diamicton also contains a number
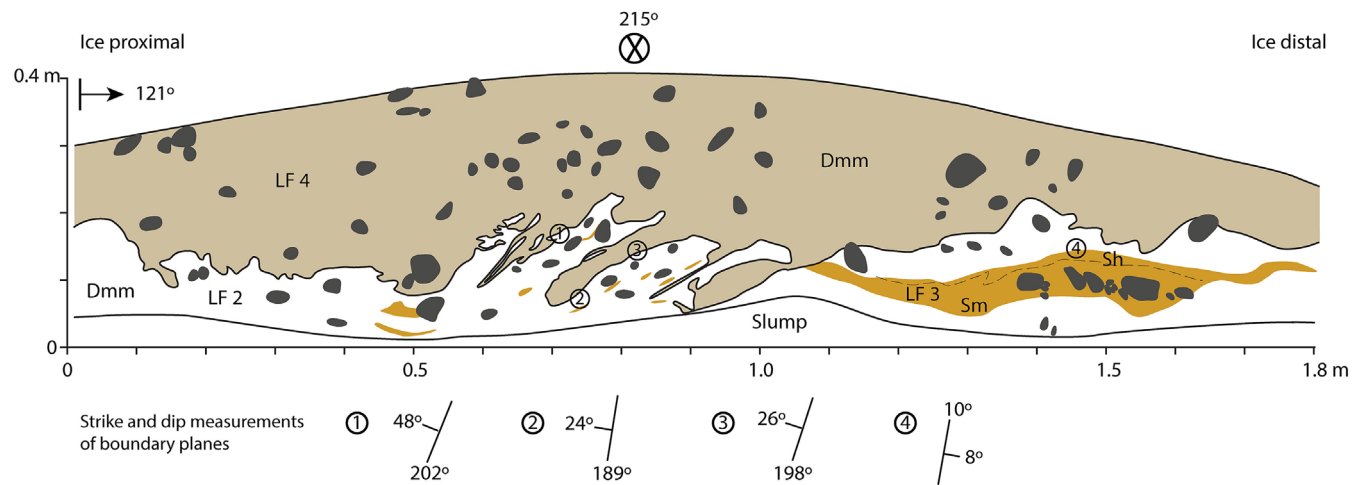
FIGURE 9 Log of section FIN-M2.

of fine sand lenses and wisps. We assign this diamicton to LF 2 based on its similarity to LF 2 in FIN-F1. A larger lens of sand (LF 3), which contains a single-layer concentration of clasts, occurs on the right of the section, close to the boundary. Towards the top of this lens, a darker sand lamination contains an overturned fold. The upper diamicton (LF 4) is massive, lighter in colour and comprises a coarse-sandy matrix with slightly less clasts. The boundary between the two diamictons is characterised by overturned folds, with axial planes that dip towards the proximal side of the moraine, stringers of LF 2 and pseudo-flame structures. Structural measurements taken at the boundary dip 24–48° and strike 189–202°, confirming that the folds limbs dip perpendicular to the crestline in an upglacier direction. In contrast, an additional measurement was taken at the upper boundary of the sand lens (LF 3) and recorded a dip of 8° and strike of 10°. The clast sample (FIN-M2b) from LF 2 is similar to that within LF 2 in FIN-F1; the clasts are relatively blocky (C_{40}:32) and angular to subrounded (RA:8; RWR:8) (Figure 7). Clasts within LF 4 (sample FIN-M2a) are similar, although slightly more angular (C_{40}:26; RA: 14; RWR: 2).

Interpretation: The lower diamicton in FIN-M2 (LF 2) is interpreted as a sub-glacial traction till (see Section 4.2.2). In contrast, the upper sandy diamicton (LF 4) is interpreted as a debris flow deposit, based on its coarser texture, lack of structure and stratigraphic context (e.g. Chandler, Chandler, et al., 2020; Chandler et al., 2016; Krüger, 1995; Lawson, 1982; Sharp, 1984; Wyshnytzky et al., 2020). We suggest that this unit was deposited by debris melt out from the ice, producing a slow-moving slurry down the moraine slopes that had sufficient water content to remove the finer particles (Lawson, 1982). An additional source of this debris may have been supraglacial debris bands close to the Fingerbreen margin. Features consistent with supraglacial debris bands can be identified on the 1968 aerial photograph (Figure 5b), and descriptions of arcuate debris bands were provided by Knudsen & Theakstone (1984). The slightly more angular clast sample within LF 4 compared with LF 2 suggests a greater supraglacial component in this diamicton. We suggest that the sand lens (LF 3) was initially laid down glaciofluvially in small streams or shallow ponds close to the ice margin (similar to the former ponds shown in Figure 4e) prior to being incorporated into the moraine (e.g. Chandler et al., 2016; Reinardy et al., 2013).

The asymmetrically folded and pseudo-flame-like boundary between LF 2 and LF 4 indicates that the sediments underwent deformation and fluid flow as a result of compression (McCarroll & Rijsdijk, 2003) under high pore water pressures (Phillips et al., 2007). The direction of asymmetry within the folds and their dip direction indicates a force from the upglacier side, commensurate with proglacial push moraine formation (Bennett, 2001; Chandler, Chandler, et al., 2020; Chandler et al., 2016; Krüger, 1994; Lukas, 2012; McCarroll & Rijsdijk, 2003). As LF 2 appears to have been folded and extruded into LF 4, the two diamictons must have been deposited prior to pushing, suggesting that a small readvance occurred after debris flow deposits from the ice margin had already been emplaced. The asymmetric fold within LF 3 demonstrates compression throughout the moraine ridge. We suggest that the downglacier-dipping structural measurement from LF 3 is part of a larger fold on the distal side, as expressed in the wavy nature of LF 3's upper boundary.

4.2.4 | Sawtooth moraine, Zone 2

Description: Section FIN-M3 (Figure 10) was cut into a sawtooth moraine, perpendicular to the crestline, at the point at which the crestline is oriented 135–315°, which is near-parallel to the main ice-flow direction. At this location, the moraine is 3.4 m wide and 0.5 m in height. The section consists predominantly of a dark silty-sandy diamicton (LF 2), which is capped by only a thin (~0.1 m thick) layer of coarse-sandy diamicton (LF 4). Similar to other sections, LF 2 contains thin sand lenses and wisps. Within the majority of the section, the sand lenses dip steeply towards the ice-proximal side but are horizontally to sub-horizontally bedded at the proximal edge and at the distal side dip both distally and proximally. Two larger lenses of sand (LF 3) occur within the section and dip parallel to the finer sand lenses. One of the large sand lenses separates LF 2 from LF 4, while the other begins at the LF 2-LF 4 boundary and descends into LF 2. Bedding within the sand lenses is horizontal to wavy, becoming convoluted in places and includes some granule layers. Structural measurements were taken at the boundaries between the sand lenses and LF 2 dip 29–65° and strike 117–144°, confirming that the sand lenses dip towards the ice-proximal side, broadly perpendicular to the moraine
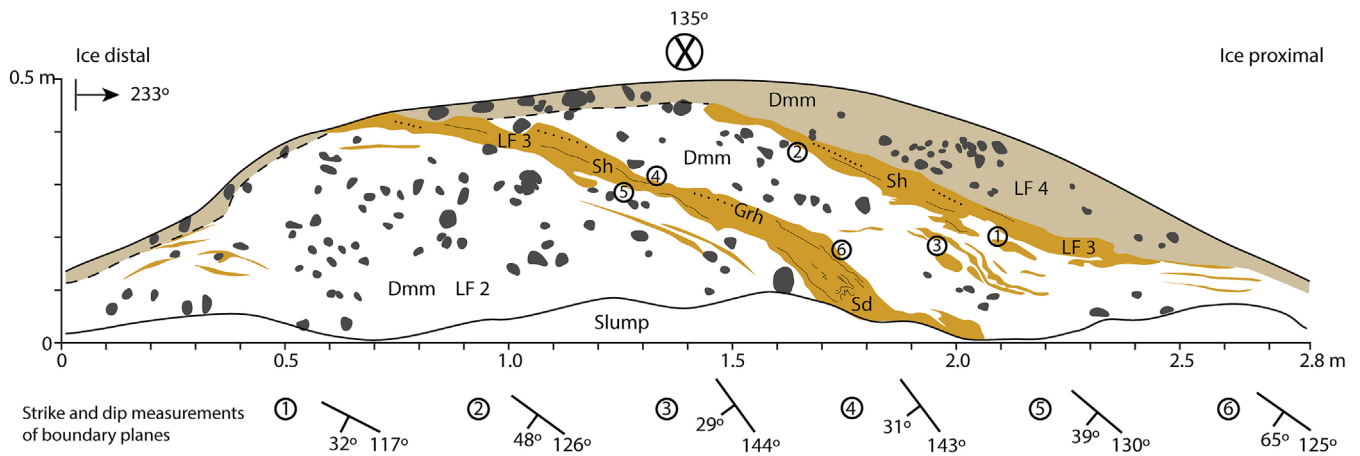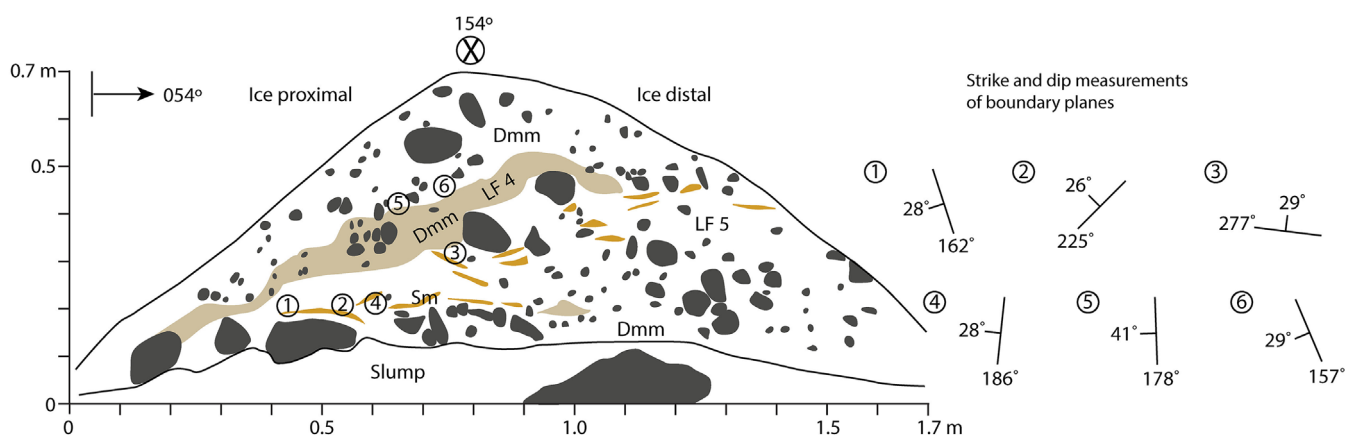
FIGURE 10   Log of section FIN-M3.

FIGURE 11   Log of section FIN-M4.

crestline. Clast shape samples from LF 2 are blocky (C₄₀: 24) and subangular to subrounded (RA: 4; RWR: 0) (Figure 7), similar to LF 2 samples from other sections.

Interpretation: LFs 2, 3 and 4 have previously been interpreted, respectively, as a sub-glacial traction till, a glaciofluvial layer and a debris flow deposit. As discussed for FIN-F1, we suggest that the finer sand lenses within LF 2 were incorporated into the sub-glacial till prior to moraine construction. In contrast, the larger sand lenses (LF 3) were likely deposited glaciofluvially in front of the ice margin.

Structurally, the steeply dipping layers of LF 3 resemble slabs of sediment that have been stacked against LF 2. We argue that this indicates a mechanism of submarginal freeze-on for moraine emplacement (e.g. Chandler et al., 2016; Evans & Hiemstra, 2005; Hiemstra et al., 2015; Krüger, 1993, 1994, 1995, 1996; Matthews et al., 1995; Reinardy et al., 2013). According to this model, we suggest that LF 3 was initially deposited proglacially in small streams or shallow ponds on top of recently exposed sub-glacial till in the previous melt-season (e.g. Figure 4g). Initial winter glacier advance overrode and incorporated the sorted sediments into the submarginal zone causing some deformation or fluidisation within the sand (Phillips et al., 2007). Submarginal freeze-on and further winter re-advance then transported the sediment slab forwards, before it was emplaced by meltout in the

spring/summer (cf. Chandler et al., 2016; Hiemstra et al., 2015; Matthews et al., 1995; Reinardy et al., 2013).

The variable visible orientations of sand lenses on the distal side of the moraine suggest some pushing of sediments in front of the ice margin during slab emplacement, producing large-scale compressional folding. On the ice-proximal side, sand lenses curve towards horizontal bedding, which could be evidence for slumping at the edge of the moraine as the ice margin receded and removed support (cf. Lukas, 2005).

4.2.5 | Lateral moraine on bedrock high, Zone 3

Description: Section FIN-M4 (Figure 11) was created in the upper metre of a 4 m high, 2 m wide, bouldery moraine, with a crestline orientation of 154–334°. The moraine is located at the top of the bedrock high within Zone 3. Compared with moraines in Zone 1 (e.g. FIN-M1; Figure 6), the moraine and others around it are narrower with sharper crestlines and more sinuous profiles, but the moraine is substantially larger than those in Zone 2. Based on aerial photographs (Table 1), moraine FIN-M4 most likely formed soon after 1985, although it is possible that the ice margin re-occupied this position
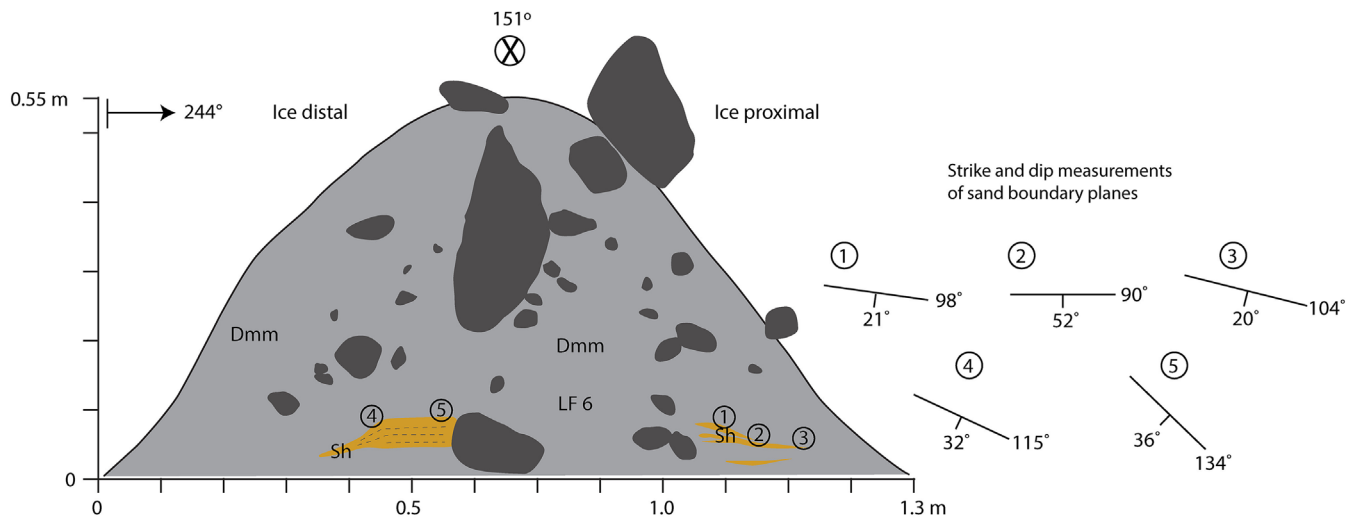
FIGURE 12   Log of section FIN-M5.

during the 1990s. The moraine is composed of a relatively loose, clast-rich, fissile, matrix-supported sandy-silty diamicton (LF 5) that contains all clast sizes up to large boulders. Some boulders are bullet-shaped and faceted. A clast sample indicates that the clasts are relatively blocky (C_{40}: 32) and are angular to subrounded (RA: 4; RWR: 0) (Figure 7). LF 5 also contains a large number of white sand lenses and wisps in the lower part of the section that generally dip in an ice-proximal direction. Four structural measurements were taken at either the upper or lower boundaries of the sand lenses and record dips of 26–29° and variable strikes of 162–277° (Figure 11). Two of these measurements dip perpendicular, and one dips parallel, to the moraine crestline, all in an upglacier direction. In contrast, a fourth measurement dips towards the distal side of the moraine.

A large body of a coarse-sandy diamicton (LF 4) occurs within LF 5 and is thickest on the ice-proximal side of the section, tapering out towards the distal side. Two structural measurements were taken at the upper boundary of the sandy diamicton lens and give dips of 29° and 41° and strikes of 157° and 178°, respectively (Figure 11), that is, the diamicton lens dips towards the ice-proximal side, perpendicular to the crestline.

Interpretation: The fissile nature of the matrix-supported sandy-silty diamicton (LF 5) and occurrence of bullet-shaped and faceted boulders is diagnostic of a sub-glacial traction till (cf. Evans, 2018; Evans et al., 2006). The clast shape and roundness sample is similar to the sub-glacial control samples, supporting this interpretation (Figure 7). Following arguments made for FIN-M2, the sandy diamicton lens (LF 4) is interpreted as a debris flow deposit (e.g. Lawson, 1982). Based on the overall structural architecture of FIN-M4, with upglacier-dipping sand and sandy diamicton lenses, we suggest that this moraine also formed through submarginal freeze-on (sensu Krüger, 1996), as discussed in Section 4.2.4.

4.2.6 | Lateral moraine on reverse bed slope, Zone 3

Section FIN-M5 was excavated into a small 0.55 m high, sharp-crested moraine ridge close to the 2016 ice margin (Figure 12). The

sediment was saturated, and the moraine is likely to have formed in 2015/2016. The moraine is composed of a massive, silty-clay diamicton (LF 6) that exhibits some fissility and is not as clast-rich as some of the other sections. A prominent faceted and bullet-shaped boulder with a vertically oriented *a*-axis occurs in the central upper part of the section, and the moraine contains other bullet-shaped clasts. Several thin sand lenses occur towards the base of the ice-proximal side and dip 20–52° and strike 90–104°; that is, they dip approximately 40° away from the crestline in an upglacier direction. A larger body of horizontally bedded sand occurs towards the centre of the section, adjoined to a large clast. Structural measurements at the upper boundary of the sand dip 32–36° and strike 115–134°, which is similar in orientation to the thin ice-proximal sand lenses. Clast shape and roundness samples taken from FIN-M5 indicate that the clasts have predominantly blocky forms (C_{40}:24) and are angular to subrounded (RA: 12; RWR:0) (Figure 7).

Interpretation: The silty-clay composition, fissility and occurrence of faceted bullet-shaped boulders within LF 6 are characteristic of a sub-glacial traction till (Evans, 2018; Evans et al., 2006). This interpretation is supported by the clast shape and roundness sample being very similar to the sub-glacial control samples. Given that the moraine is predominantly composed of sub-glacial till and lacking in any large-scale structures, we suggest that moraine formation was through squeezing up of a viscous slurry of saturated sediments at and immediately beneath the ice margin during winter ice advance (Chandler, Chandler, et al., 2020; Chandler et al., 2016; Price, 1970; Sharp, 1984). The sand lenses at the base of the moraine were likely incorporated from pre-existing sorted sediments immediately in front of the ice margin (e.g. Figure 4g).

5 | DISCUSSION

5.1 | Zone 1: Efficient meltwater drainage

At the LIA maximum and during initial stages of recession, a striking asymmetry in moraine characteristics across the valley sides is apparent. While large boulder-covered, matrix-supported moraines formed

on the southwestern valley side, the northeastern valley side is characterised by boulder lines and bouldery moraines devoid of finer grained material (Figure 4a). This suggests higher glaciofluvial activity on the northeastern side that flushed out finer grained sediment (cf. Winkler, 2021). This assertion is supported by the presence of a still active prominent tributary to the main channel on the northeastern side, 300–400 m from the LIA limit, that follows the shape of lateral–frontal moraines and would have flowed around the former ice margin, efficiently removing glaciogenic debris (Benn et al., 2003). A large meltwater portal likely existed on this side of the ice margin, as can be seen in 1957 (Figure 5a) and indicated by the two eskers and large former channel to the east of Zone 2. The difference in glaciofluvial activity in this area may be a result of differences in the insolation received by each side of the foreland, with enhanced melt on the sunnier northeastern side of the valley (cf. Chandler et al., 2021; Thome, 1972).

As recession progressed, meltwater became more concentrated in the valley centre incising down into the bedrock. Further upvalley, steeper bedrock on the northeastern valley side caused the main channel to switch to a braided network of channels on the southwestern valley floor, prohibiting moraine formation in this area. Proglacial channel patterns have typically been linked to changes in sediment supply and discharge rates (e.g. Gurnell et al., 2000; Staines et al., 2015). However, Marren and Toomath (2014) demonstrate the importance of topography for determining proglacial channel patterns. At Fingerbreen, changes in topography as a result of bedrock undulations have clearly influenced the route of meltwater drainage, in turn influencing the type of ice-marginal zone sediments and therefore moraine composition. The lateral moraine FIN-M1, which formed a few years prior to 1957, is composed of glaciofluvial sediments that have been pushed by the ice margin into a moraine ridge. The location of the moraine within a large-scale hollow in the bedrock indicates that meltwater flow in this area from the northern portal (Figure 5a,b) was likely guided around the ice margin against the valley side. The lack of finer grained sediment indicates that the meltwater drained freely, efficiently removing finer material.

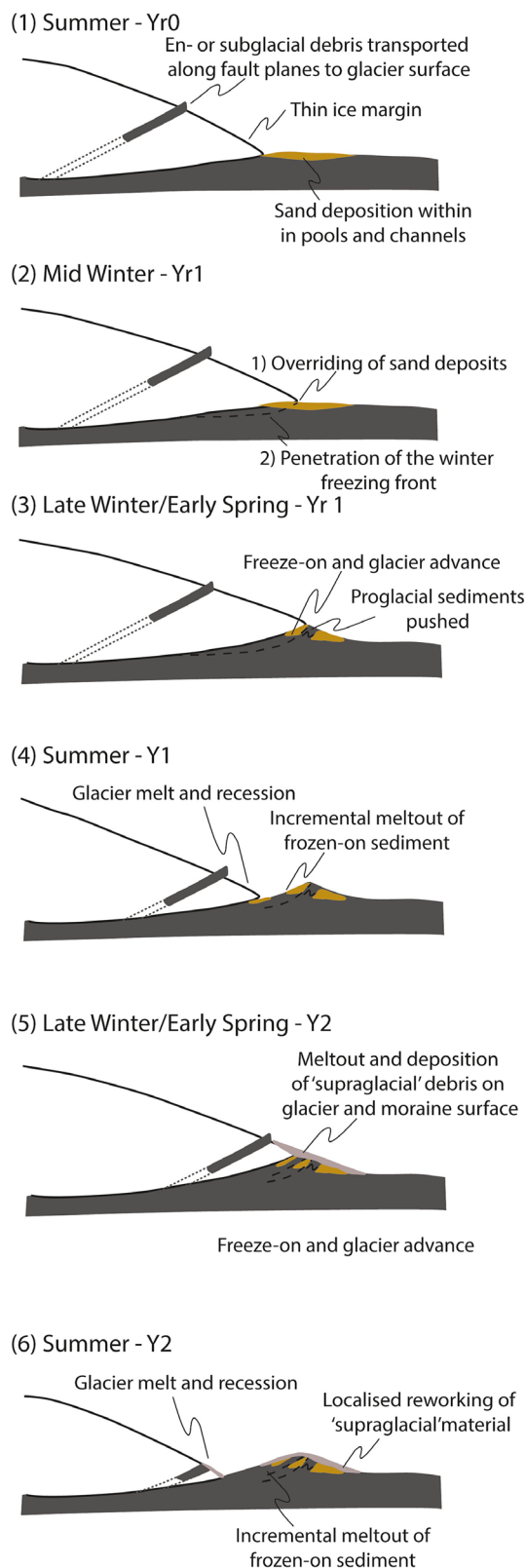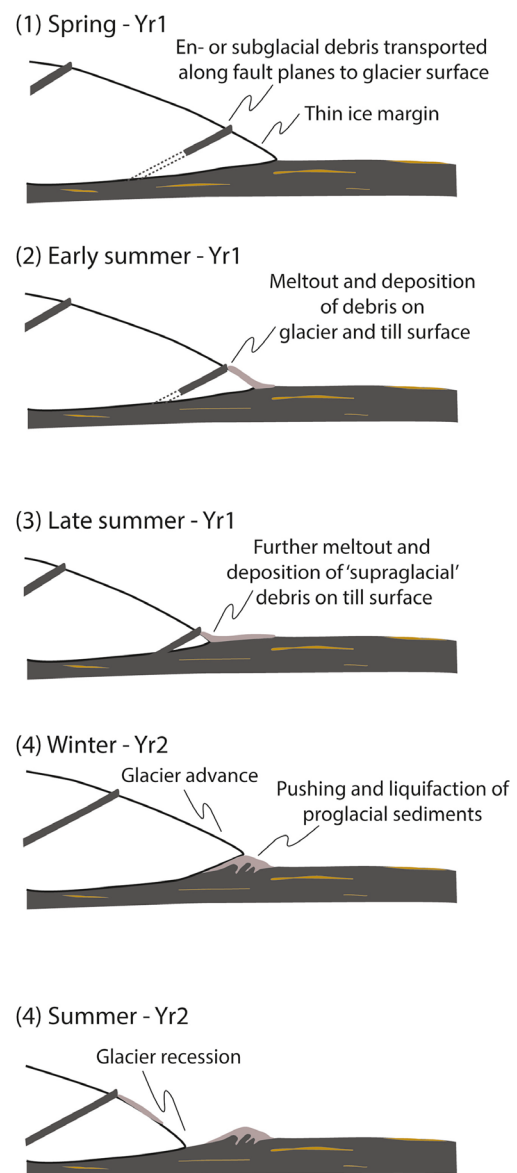## 5.2 | Zone 2: Inefficient meltwater drainage and changes in glacier structure

In contrast to Zone 1, Zone 2 represents an area of inefficient meltwater drainage (Benn et al., 2003). The location of meltwater portals to the north and south ensured the preservation of this zone in the central interfluve (Figure 5a,b). Later in recession, meltwater on the northeastern valley side appears to have been diverted across the ice-proximal side of Zone 3 by the bedrock high (Figure 5c), helping to consolidate drainage within the main channel rather than being distributed across the foreland. Zone 2 was 'water-soaked' in the 1960s and 1970s (Knudsen & Theakstone, 1984, p.379) (Figure 5b), which influenced processes of moraine formation as discussed further below.

The change from transverse moraines to sawtooth moraines within this zone represents a transition in the structure of the ice margin, as previously observed by Knudsen and Theakstone (1984). In the 1957 and 1968 aerial photographs, the ice margin is arcuate, but by 1985, the frontal zone is more intensely crevassed, forming

ice 'pecten' between longitudinal crevasses (cf. Evans et al., 2016) (Figure 5). This structural transformation has been observed at a number of Icelandic glaciers in recent decades (e.g. Fláajökull, Skálafellsjökull, Fjallsjökull, Skaftafellsjökull and Svínafellsjökull) and has been associated with thinning ice margins receding into over-deepenings (e.g. Chandler et al., 2016; Chandler, Evans, et al., 2020; Evans et al., 2016, 2017; Everest et al., 2017; Jónsson et al., 2016; Lee et al., 2018). Conversely, at Fingerbreen, the transition that occurred is likely the result of the thinning ice margin becoming increasingly influenced by the upglacier bedrock high. The spatial arrangement of the flutes and sawtooth moraines, with flutes occurring on the ice-proximal slopes of the moraines (Figure 4e), suggests that the flutes are genetically linked to the sawtooth moraines, forming during the same advance (Chandler, Evans, et al., 2020; Evans & Twigg, 2002). Conversely, the transverse moraines were overlain over more continuous flutes as described elsewhere in Norway (e.g. Worsley, 1974).

The formation of flutes beneath temperate glaciers is most commonly attributed to converging flow of till around a lodged boulder into its lee-side cavity, which then propagates downglacier (Benn, 1994; Boulton, 1976; Ely et al., 2017; Evans et al., 2010). Ives and Iverson (2019) suggest that unsteady pore water pressure conditions are required for flutes to extend beyond the pressure shadow of the initiating boulder. These authors advocate a cycle of initial high sub-glacial water pressure and slip velocity, which squeezes till into cavities, followed by a reduction in water pressure and slip velocity. This allows an increase in ice pressure and consolidation of the newly accreted till in the flute, enabling cavity formation during the next phase of high-water pressure. We suggest that the thin horizontally bedded sand lenses within section FIN-F1 (Section 4.2.2) were deposited during this cyclical process of flute formation as a result of fluctuating pore water pressures. Despite the relatively high hydraulic permeability of the diamicton due to the sand content, the evidence for fluid flow within moraines (e.g. FIN-M2) indicates poor sub- and ice-marginal drainage conditions (Evans et al., 2010), as observed at the time (Knudsen & Theakstone, 1984).

The combination of a saturated proglacial area and thin ice margin also provided favourable conditions for submarginal freeze-on (cf. Chandler et al., 2016; Reinardy et al., 2019). We suggest that across this area of the foreland, drainage conditions and associated moraine-forming processes varied both spatially and annually (Figure 13). In colder winters, penetration of the freezing front below the ice margin led to freeze-on of submarginal sediments, sometimes containing overridden glaciofluvial material (e.g. Chandler et al., 2016). In other years, or in other parts of the ice margin, a saturated proglacial area with high porewater pressures led to till squeezing and bulldozing at the margin and around ice pecten (e.g. Chandler et al., 2016; Chandler, Evans, et al., 2020; Chandler, Lukas, & Boston, 2020; Evans et al., 2016, 2017). The two well-defined sediment slabs in FIN-M3 could imply that the sawtooth moraine formed over at least 2 years (e.g. Hiemstra et al., 2015) (Figure 12). Alternatively, multiple slabs that were likely produced during a single year have been recognised at other sites (Chandler et al., 2016). A freeze-on mechanism for moraine formation has been identified at several sites in Norway and Iceland (e.g. Chandler et al., 2016; Evans & Hiemstra, 2005; Hiemstra et al., 2015; Krüger,

(a) Submarginal freeze-on

(1) Summer - Yr0

En- or subglacial debris transported along fault planes to glacier surface

Thin ice margin

Sand deposition within in pools and channels

(2) Mid Winter - Yr1

1) Overriding of sand deposits

2) Penetration of the winter freezing front

(3) Late Winter/Early Spring - Yr 1

Freeze-on and glacier advance

Proglacial sediments pushed

(4) Summer - Y1

Glacier melt and recession

Incremental meltout of frozen-on sediment

(5) Late Winter/Early Spring - Y2

Meltout and deposition of 'supraglacial' debris on glacier and moraine surface

Freeze-on and glacier advance

(6) Summer - Y2

Glacier melt and recession

Localised reworking of 'supraglacial' material

Incremental meltout of frozen-on sediment

(b) Pushing and proglacial defomation

(1) Spring - Yr1

En- or subglacial debris transported along fault planes to glacier surface

Thin ice margin

(2) Early summer - Yr1

Meltout and deposition of debris on glacier and till surface

(3) Late summer - Yr1

Further meltout and deposition of 'supraglacial' debris on till surface

(4) Winter - Yr2

Glacier advance

Pushing and liquifaction of proglacial sediments

(4) Summer - Yr2

Glacier recession

FIGURE 13 Schematic models of processes of annual moraine formation at transverse and sawtooth moraines in the Fingerbreen foreland by (a) submarginal freeze-on and (b) pushing and proglacial defomation.

1993, 1994, 1995, 1996; Matthews et al., 1995; Reinardy et al., 2013). However, it has rarely been recognised as contributing to sawtooth moraine development, where till squeezing around the ice-marginal pecten and within longitudinal crevasses is often

advocated (e.g. Chandler, Evans, et al., 2020; Chandler, Lukas, & Boston, 2020; Evans et al., 2016).

In the downvalley part of Zone 2, we count more transverse moraines than years between 1957 and 1968, implying that some sub-

annual moraines are present. Sub-annual moraines have been rarely documented in the literature (e.g. Chandler et al., 2016; Chandler, Evans, et al., 2020) but are thought to occur in situations where squeeze-push mechanisms become decoupled over a seasonal cycle. In these cases, strong summer glacier retreat enables (multiple) squeeze moraines to be formed in between winter push moraines, rather than a single composite push-squeeze moraine being constructed (Chandler, Evans, et al., 2020; Chandler, Lukas, & Boston, 2020).
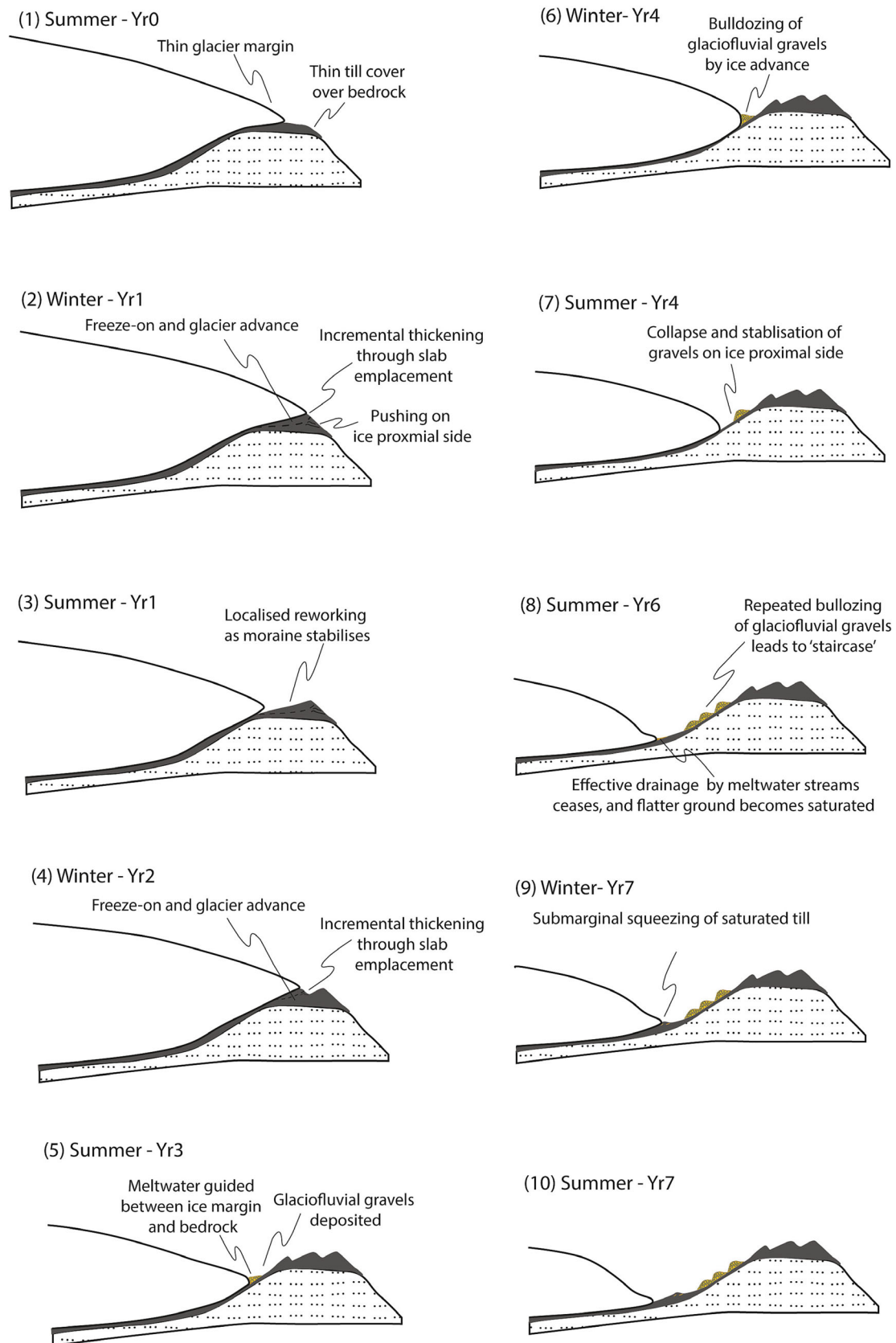
FIGURE 14 Schematic model of processes of moraine formation on top of and on the reverse-bed slope of a bedrock high in the Fingerbreen foreland over an undefined number of years.

5.3 | Zone 3: Changing drainage conditions and ice-flow dynamics on a reverse-bed slope

The landform-sediment assemblages in Zone 3 are controlled by the bedrock high on the northeastern valley side. Given that there are few moraines in the area between the 1985 and 2002 glacier margins (which are at the downvalley and upvalley sides of the bedrock high respectively), the bedrock high likely acted as a pinning point (cf. Rowan et al., 2022), resulting in a set of closely spaced, bifurcating moraines that probably formed over several years or were reoccupied. The time frame coincides with a period in the 1990s when glaciers in Norway readvanced (Andreassen et al., 2005; Chinn et al., 2005), which would have also contributed to a slower overall recession rate and reoccupation of moraines. A thin glacier margin over the bedrock high would have provided favourable conditions for the freeze-on of submarginal sediment slabs (e.g. Krüger, 1996) (Figure 14). The bedrock high also contributed to the preservation of these moraines because it diverted meltwater exiting from the northern side of Fingerbreen southwards around the ice margin before joining the main channel.

The clast-supported nature of moraines on the reverse bedrock slope indicates that as glacier recession progressed, sediments deposited in ice-marginal meltwater channels were subsequently bulldozed into moraines, similar to moraines in Zone 1 (e.g. FIN-M1). It is likely that finer grained material from sub- and englacial sources was removed and redistributed by this lateral meltwater. In 2016, the ice margin had reached a flatter area and drainage was again restricted due to the reverse slope acting as a barrier, and because Fingerbreen by then was receding into a larger overdeepening, similar to many glaciers in Iceland (e.g. Chandler, Chandler, et al., 2020; Chandler, Evans, et al., 2020; Evans et al., 2016, 2019; Everest et al., 2017; Guðmundsson & Evans, 2022; Jónsson et al., 2016; Lee et al., 2018; Schomacker, 2010). This caused a saturated ice margin, resulting in squeezing up of a silty-clay sub-glacial till into small moraine ridges (Price, 1970). The abundance of ice-cored sand ridges that emanate from longitudinal crevasses also indicates areas of restricted drainage where evacuation of englacial drainage channels within the ice has been restricted, forming small eskers or kames, some of which may have been later bulldozed by the ice margin.

5.4 | Topographic controls on glacier dynamics and landform development

The sequence of events described for the three zones highlights the importance of topography in moraine spacing, process of moraine formation, drainage conditions at the ice margin and preservation potential. The bedrock high on the northeastern valley side has exerted a strong control on the suite of landform-sediment assemblages deposited from the 1970s onwards. This bedrock high has influenced processes of moraine formation by the following: (a) causing thinning downglacier between 1968 and 1985 that resulted in increased longitudinal crevassing, causing the development of ice pectination and resulting in a switch from straight transverse frontal moraines to sawtooth moraines (e.g. Evans et al., 2016); (b) diverting the northern meltwater channel towards the south, either sub- or ice-marginally, allowing Zone 2 (the area of transverse and sawtooth moraines) to be preserved; (c) acting as a pinning point during the late 1980s and 1990s that resulted in few moraines being deposited during this time; (d) causing a thin glacier margin over it that provided favourable conditions for moraine formation via freeze-on of submarginal sediment slabs to the glacier bed; and (e) directing meltwater flow southwards around the ice margin, as Fingerbreen receded down the reverse slope, resulting in cobble terraces and bulldozing of this glaciofluvial material by winter ice advance.

There are some similarities between the landform-sediment signatures of Fingerbreen and glaciers in southern Iceland, which are also currently receding into overdeepenings. However, unlike at the Icelandic glaciers (e.g. Chandler, Evans, et al., 2020; Evans et al., 2016), the bedrock high at Fingerbreen has also been strongly influential. Chandler et al. (2016) discuss how moraines deposited at Skàlafellsjökull have influenced drainage pathways across the foreland, while at Fingerbreen, the topography of the valley has been a stronger control on meltwater flow (Marren & Toomath, 2014). Similar to Midtdalsbreen in Norway, thinning of the ice margin and a saturated ice-marginal zone led to moraine emplacement through freeze-on of submarginal sediment slabs (Reinardy et al., 2013, 2019). Continued recession into the overdeepening is likely to result in lake-level lowering and incision in the area close to the ice margin (Marren & Toomath, 2013).

The role of topography in moraine spacing has been widely discussed (e.g. Oerlemans, 2012; Pedersen & Egholm, 2013; Barr & Lovell, 2014; Boston & Lukas, 2019; Magrani et al., 2021; Rowan et al., 2022), and this study provides a detailed example of how undulations in glacier foreland topography affect drainage patterns and the distribution and preservation potential of moraines. Firstly, continued glacier recession across the relatively flat Zone 2 provided the conditions for annual, and some sub-annual, moraine development. Secondly, the interplay between climatically driven glaciological changes (positive mass balance years during the 1990s; Andreassen et al., 2005) and topography (the bedrock high, which acted as a pinning point) resulted in fewer but larger moraines being constructed between 1985 and 2002. This corroborates modelling by Rowan et al. (2022) that the largest moraines form at pinning points and that moraine spacing is larger on flatter slopes (Oerlemans, 2012). Our work at Fingerbreen demonstrates the need to take even relatively small-scale bedrock undulations in the glacier foreland into consideration in any moraine-based palaeoclimate studies.

Processes of moraine formation have also been used in palaeoglacial research to infer glacier dynamics (e.g. Chandler, Lukas, & Boston, 2020; Lukas, 2005). Here, we demonstrate spatial variability in moraine-forming processes within a relatively small area due to changes in sub- and ice-marginal topography and drainage conditions. We show large differences in moraine composition, from clast-supported sandy diamicton to silty-clay diamicton, over a short distance as a result of changing drainage efficiency at the ice margin caused by changes in slope. We recommend that bedrock topographic factors that may affect ice margin morphology and structure and ice-marginal drainage conditions should be considered in any assessment of glacier dynamics.

6 | CONCLUSIONS

We present the LIA to present day geomorphological and sedimentological record of Fingerbreen, an outlet glacier of the Østre Svartisen

plateau icefield. We divide the foreland into three zones. Zone 1 includes the LIA limit and is characterised by bouldery moraines interspersed by areas of striated bedrock. Zone 2 is a flat area of heavily fluted terrain, with cross-cutting annual, and some sub-annual, transverse and sawtooth moraines, that became exposed between 1957 and 1985. Here, a switch occurred during the 1970s from transverse to sawtooth moraines as a result of changes in the morphology and structure of the ice margin. Since 1985, Fingerbreen has been receding over and down the reverse slope of a bedrock high on the northern valley side (Zone 3).

Section logs for five representative moraines and one flute, located across the three zones, were examined. The sedimentological analysis reveals three main types of moraine-forming processes that changed as ice margin morphology and structure evolved, influenced by foreland topography. Firstly, moraines formed through push and bulldozing of pre-existing sediments. There are several examples of this: (i) At the lateral margin in the 1940s to 1950s (Zone 1), and on the reverse-bed slope in the 2000s (Zone 3), glaciofluvial sediments were deposited between the ice margin and valley side or reverse slope and were subsequently deformed during minor glacier advance; (ii) in the fluted Zone 2, a cross-cutting transverse moraine was constructed through push of saturated pre-existing sediments (sub-glacial till and supraglacial debris flow deposits) leading to folding and fluidised flow. Secondly, we show evidence for squeezing of saturated sub-glacial till into small (∼0.4 m) moraine ridges at the base of the reverse-bed slope (Zone 3) (∼2014–2016). Thirdly, where the ice margin was thin, moraine formation occurred through submarginal freeze-on of sub-glacial till and pre-existing ice-marginal sediments. Evidence for this was found in a 1970s sawtooth moraine in Zone 2 and in moraines on top of the bedrock high.

The spatial and temporal variability in moraine-forming processes at the glacier margin demonstrates that valley topography exerts a strong influence on ice margin shape and structure, and meltwater flow pathways, which in turn controls moraine formation processes. This work demonstrates the key role of foreland topography in moraine spacing and processes of moraine formation, which needs to be taken into consideration when using moraines to make inferences about palaeoclimate and glacier dynamics.

CONFLICT OF INTEREST STATEMENT

The authors declare that they have no conflict of interest.

DATA AVAILABILITY STATEMENT

The data that support the findings of this study are available from the corresponding author upon reasonable request.

ORCID

Clare M. Boston https://orcid.org/0000-0002-8973-5366
Benjamin M. P. Chandler https://orcid.org/0000-0003-1532-9696
Harold Lovell https://orcid.org/0000-0002-9435-3178
Paul Weber https://orcid.org/0000-0002-1623-9126
Bethan J. Davies https://orcid.org/0000-0002-8636-1813

REFERENCES

Andreassen, L.M., Elvehøy, H., Kjøllmoen, B. & Belart, J.M. (2020) Glacier change in Norway since the 1960s—an overview of mass balance, area, length and surface elevation changes. *Journal of Glaciology*, 66(256), 313–328. Available from: https://doi.org/10.1017/jog.2020.10

Andreassen, L.M., Elvehøy, H., Kjøllmoen, B. & Engeset, R.V. (2005) Glacier mass-balance and length variation in Norway. *Annals of Glaciology*, 42, 317–325. Available from: https://doi.org/10.3189/172756405781812826

Andreassen, L.M., Nagy, T., Kjøllmoen, B. & Leigh, J.R. (2022) An inventory of Norway's glaciers and ice-marginal lakes from 2018–19 Sentinel-2 data. *Journal of Glaciology*, 68(272), 1085–1106. Available from: https://doi.org/10.1017/jog.2022.20

Antoniazza, G. & Lane, S.N. (2021) Sediment yield over glacial cycles: a conceptual model. *Progress in Physical Geography: Earth and Environment*, 45(6), 842–865. Available from: https://doi.org/10.1177/0309133321997292

Barr, I.D. & Lovell, H. (2014) A review of topographic controls on moraine distribution. *Geomorphology*, 226, 44–64. Available from: https://doi.org/10.1016/j.geomorph.2014.07.030

Beniston, M., Farinotti, D., Stoffel, M., Andreassen, L.M., Coppola, E., Eckert, N. et al. (2018) The European mountain cryosphere: a review of its current state, trends, and future challenges. *The Cryosphere*, 12(2), 759–794. Available from: https://doi.org/10.5194/tc-12-759-2018

Benn, D.I. (1994) Fluted moraine formation and till genesis below a temperate valley glacier: Slettmarkbreen, Jotunheimen, southern Norway. *Sedimentology*, 41(2), 279–292. Available from: https://doi.org/10.1111/j.1365-3091.1994.tb01406.x

Benn, D.I., Kirkbride, M.P., Owen, L.A. & Brazier, V. (2003) Glaciated valley landsystems. In: Evans, D.J.A. (Ed.) *Glacial landsystems*. London, New York: Routledge, pp. 372–406.

Bennett, M.R. (2001) The morphology, structural evolution and significance of push moraines. *Earth-Science Reviews*, 53(3-4), 197–236. Available from: https://doi.org/10.1016/S0012-8252(00)00039-8

Boston, C.M. & Lukas, S. (2019) Topographic controls on plateau icefield recession: insights from the younger Dryas Monadhliath icefield, Scotland. *Journal of Quaternary Science*, 34(6), 433–451. Available from: https://doi.org/10.1002/jqs.3111

Boston, C.M., Lukas, S. & Carr, S.J. (2015) A younger Dryas plateau icefield in the Monadhliath, Scotland, and implications for regional palaeoclimate. *Quaternary Science Reviews*, 108, 139–162. Available from: https://doi.org/10.1016/j.quascirev.2014.11.020

Boulton, G.S. (1976) The origin of glacially fluted surfaces: observations and theory. *Journal of Glaciology*, 17(76), 287–309. Available from: https://doi.org/10.3189/S0022143000013605

Carrivick, J.L., Andreassen, L.M., Nesje, A. & Yde, J.C. (2022) A reconstruction of Jostedalsbreen during the Little Ice Age and geometric changes to outlet glaciers since then. *Quaternary Science Reviews*, 284, 107501. Available from: https://doi.org/10.1016/j.quascirev.2022.107501

Carrivick, J.L., Boston, C.M., King, O., James, W.H., Quincey, D.J., Smith, M.W. et al. (2019) Accelerated volume loss in glacier ablation zones of NE Greenland, Little Ice Age to present. *Geophysical*

Research Letters, 46(3), 1476–1484. Available from: https://doi.org/10.1029/2018GL081383

Chandler, B.M.P., Boston, C.M., Lukas, S. & Lovell, H. (2021) Re-interpretation of 'hummocky moraine' in the Gaick, Scotland, as erosional remnants: implications for palaeoglacier dynamics. *Proceedings of the Geologists' Association*, 132(4), 506–524. Available from: https://doi.org/10.1016/j.pgeola.2021.06.002

Chandler, B.M.P., Chandler, S.J.P., Evans, D.J.A., Ewertowski, M.W., Lovell, H., Roberts, D.H. et al. (2020) Sub-annual moraine formation at an active temperate Icelandic glacier. *Earth Surface Processes and Landforms*, 45(7), 1622–1643. Available from: https://doi.org/10.1002/esp.4835

Chandler, B.M.P., Evans, D.J.A., Chandler, S.J.P., Ewertowski, M.W., Lovell, H., Roberts, D.H. et al. (2020) The glacial landsystem of Fjallsjökull, Iceland: spatial and temporal evolution of process-form regimes at an active temperate glacier. *Geomorphology*, 361, 107192. Available from: https://doi.org/10.1016/j.geomorph.2020.107192

Chandler, B.M.P., Evans, D.J.A. & Roberts, D.H. (2016) Characteristics of recessional moraines at a temperate glacier in SE Iceland: insights into patterns, rates and drivers of glacier retreat. *Quaternary Science Reviews*, 135, 171–205. Available from: https://doi.org/10.1007/s41063-016-0024-1

Chandler, B.M.P., Lovell, H., Boston, C.M., Lukas, S., Barr, I.D., Benediktsson, Í.Ö. et al. (2018) Glacial geomorphological mapping: a review of approaches and frameworks for best practice. *Earth-Science Reviews*, 185, 806–846. Available from: https://doi.org/10.1016/j.earscirev.2018.07.015

Chandler, B.M.P., Lukas, S. & Boston, C.M. (2020) Processes of 'hummocky moraine' formation in the Gaick, Scotland: insights into the ice-marginal dynamics of a younger Dryas plateau icefield. *Boreas*, 49(2), 248–268. Available from: https://doi.org/10.1111/bor.12426

Chinn, T., Winkler, S., Salinger, M.J. & Haakensen, N. (2005) Recent glacier advances in Norway and New Zealand: a comparison of their glaciological and meteorological causes. *Geografiska Annaler. Series a, Physical Geography*, 87(1), 141–157. Available from: https://doi.org/10.1111/j.0435-3676.2005.00249.x

Davies, B., Bendle, J., Carrivick, J., McNabb, R., McNeil, C., Pelto, M. et al. (2022) Topographic controls on ice flow and recession for Juneau Icefield (Alaska/British Columbia). *Earth Surface Processes and Landforms*, 47(9), 2357–2390. Available from: https://doi.org/10.1002/esp.5383

Ely, J.C., Graham, C., Barr, I.D., Rea, B.R., Spagnolo, M. & Evans, J. (2017) Using UAV acquired photography and structure from motion techniques for studying glacier landforms: application to the glacial flutes at Isfallsglaciären. *Earth Surface Processes and Landforms*, 42(6), 877–888. Available from: https://doi.org/10.1002/esp.4044

Evans, D.J.A. (Ed). (2003) *Glacial landsystems*. London, New York: Routledge.

Evans, D.J.A. (2018) *Till: a glacial process sedimentology*. Chichester: John Wiley & Sons.

Evans, D.J.A. & Benn, D.I. (2021) *A practical guide to the study of glacial sediments*. London: Quaternary Research Association.

Evans, D.J.A., Ewertowski, M. & Orton, C. (2016) Fláajökull (north lobe), Iceland: active temperate piedmont lobe glacial landsystem. *Journal of Maps*, 12(5), 777–789. Available from: https://doi.org/10.1080/17445647.2015.1073185

Evans, D.J.A., Ewertowski, M. & Orton, C. (2019) The glacial landsystem of Hoffellsjökull, Iceland: contrasting geomorphological signatures of active temperate glacier recession driven by ice lobe and bed morphology. *SE Geografiska Annaler: Series A Physical Geography*, 101(3), 249–276. Available from: https://doi.org/10.1080/04353676.2019.1631608

Evans, D.J.A. & Hiemstra, J.F. (2005) Till deposition by glacier submarginal, incremental thickening. *Earth Surface Processes and Landforms*, 30(13), 1633–1662. Available from: https://doi.org/10.1002/esp.1224

Evans, D.J.A., Nelson, C.D. & Webb, C. (2010) An assessment of fluting and "till esker" formation on the foreland of Sandfellsjökull, Iceland. *Geomorphology*, 114(3), 453–465. Available from: https://doi.org/10.1016/j.geomorph.2009.08.016

Evans, D.J.A., Phillips, E.R., Hiemstra, J.F. & Auton, C.A. (2006) Subglacial till: formation, sedimentary characteristics and classification. *Earth-Science Reviews*, 78(1–2), 115–176. Available from: https://doi.org/10.1016/j.earscirev.2006.04.001Get

Evans, D.J.A., Roberts, D.H., Hiemstra, J.F., Nye, K.M., Wright, H. & Steer, A. (2018) Submarginal debris transport and till formation in active temperate glacier systems: the Southeast Iceland type locality. *Quaternary Science Reviews*, 195, 72–108. Available from: https://doi.org/10.1016/j.quascirev.2018.07.002

Evans, D.J.A. & Twigg, D.R. (2002) The active temperate glacial landsystem: a model based on Breiðamerkurjökull and Fjallsjökull, Iceland. *Quaternary Science Reviews*, 21(20–22), 2143–2177. Available from: https://doi.org/10.1016/S0277-3791(02)00019-7

Everest, J., Bradwell, T., Jones, L. & Hughes, L. (2017) The geomorphology of Svínafellsjökull and Virkisjökull-Falljökull glacier forelands, southeast Iceland. *Journal of Maps*, 13(2), 936–945. Available from: https://doi.org/10.1080/17445647.2017.1407272

Evans, D.J.A., Ewertowski, M. & Orton, C. (2017) Skaftafellsjökull, Iceland: glacial geomorphology recording glacier recession since the Little Ice Age. *Journal of Maps*, 13(2), 358–368. Available from: https://doi.org/10.1080/17445647.2017.1310676

Giesen, R.H. & Oerlemans, J. (2010) Response of the ice cap Hardangerjøkulen in southern Norway to the 20th and 21st century climates. *The Cryosphere*, 4(2), 191–213. Available from: https://doi.org/10.5194/tc-4-191-2010

Graham, D.J. & Midgley, N.G. (2000) Graphical representation of particle shape using triangular diagrams: an excel spreadsheet method. *Earth Surface Processes and Landforms*, 25(13), 1473–1477. Available from: https://doi.org/10.1002/1096-9837(200012)25:13<1473::AID-ESP158>3.0.CO;2-C

Guðmundsson, S. & Evans, D.J.A. (2022) Geomorphological map of Breiðamerkursandur 2018: the historical evolution of an active temperate glacier foreland. *Geografiska Annaler. Series A, Physical Geography*, 104(4), 298–332. Available from: https://doi.org/10.1080/04353676.2022.2148083

Gurnell, A.M., Edwards, P.J., Petts, G.E. & Ward, J.V. (2000) A conceptual model for alpine proglacial river channel evolution under changing climatic conditions. *Catena*, 38(3), 223–242. Available from: https://doi.org/10.1016/S0341-8162(99)00069-7

Gurney, S.D. & White, K. (2005) Sediment magnetic properties of glacial till deposited since the Little Ice Age maximum for selected glaciers at Svartisen and Okstindan, northern Norway. *Boreas*, 34(1), 75–83. Available from: https://doi.org/10.1111/j.1502-3885.2005.tb01006.x

Haeberli, W., Hoelzle, M., Paul, F. & Zemp, M. (2007) Integrated monitoring of mountain glaciers as key indicators of global climate change: the European Alps. *Annals of Glaciology*, 46, 150–160. Available from: https://doi.org/10.3189/172756407782871512

Hiemstra, J.F., Matthews, J.A., Evans, D.J.A. & Owen, G. (2015) Sediment fingerprinting and the mode of formation of singular and composite annual moraine ridges at two glacier margins, Jotunheimen, southern Norway. *The Holocene*, 25(11), 1772–1785. Available from: https://doi.org/10.1177/0959683615591359

Hiemstra, J.F., Young, G.H., Loader, N.J. & Gordon, P.R. (2022) Interrogating glacier mass balance response to climatic change since the Little Ice Age: reconstructions for the Jotunheimen region, southern Norway. *Boreas*, 51(2), 350–363. Available from: https://doi.org/10.1111/bor.12562

Holtedahl, O. (Ed). (1960) Geology of Norway. In: *Norges Geologiske Undersøkelse*, vol. 208. Oslo, Hos H. Aschehoug.

Hugonnet, R., McNabb, R., Berthier, E., Menounos, B., Nuth, C., Girod, L. et al. (2021) Accelerated global glacier mass loss in the early twenty-first century. *Nature*, 592(7856), 726–731. Available from: https://doi.org/10.1038/s41586-021-03436-z

Immerzeel, W.W., Lutz, A.F., Andrade, M., Bahl, A., Biemans, H., Bolch, T., et al. (2020) Importance and vulnerability of the world's water towers. *Nature*, 577(7790), 364–369. Available from: https://doi.org/10.1038/s41586-019-1822-y

Ives, L.R.W. & Iverson, N.R. (2019) Genesis of glacial flutes inferred from observations at Múlajökull, Iceland. *Geology*, 47(5), 387–390. Available from: https://doi.org/10.1130/G45714.1

Jónsson, S.A., Benediktsson, Í.Ö., Ingólfsson, Ó., Schomacker, A., Bergsdóttir, H.L., Jacobson, W.R. et al. (2016) Submarginal drumlin formation and late Holocene history of Fláajökull, southeast Iceland. *Annals of Glaciology*, 57(72), 128–141. Available from: https://doi.org/10.1017/aog.2016.4

Kessler, T.C., Klint, K.E.S., Nilsson, B. & Bjerg, P.L. (2012) Characterization of sand lenses embedded in tills. *Quaternary Science Reviews*, 53, 55–71. Available from: https://doi.org/10.1016/j.quascirev.2012.08.011

Knudsen, N.T. & Theakstone, W.H. (1984) Recent changes of some glaciers of East Svartisen, Norway. *Geografiska Annaler. Series A, Physical Geography*, 66(4), 367–380. Available from: https://doi.org/10.1080/04353676.1984.11880122

Krüger, J. (1993) Moraine-ridge formation along a stationary ice front in Iceland. *Boreas*, 22(2), 101–109. Available from: https://doi.org/10.1111/j.1502-3885.1993.tb00169.x

Krüger, J. (1994) *Glacial processes, sediments, landforms, and stratigraphy in the terminus region of Myrdalsjokull, Iceland*, Vol. XXI. København, Hans Reitzels Forlag, 233 pp.

Krüger, J. (1995) Origin, chronology and climatological significance of annual-moraine ridges at Myrdalsjökull, Iceland. *The Holocene*, 5(4), 420–427. Available from: https://doi.org/10.1177/095968369500500404

Krüger, J. (1996) Moraine ridges formed from subglacial frozen-on sediment slabs and their differentiation from push moraines. *Boreas*, 25(1), 57–64. Available from: https://doi.org/10.1111/j.1502-3885.1996.tb00835.x

Krzyszkowski, D. & Zieliński, T. (2002) The Pleistocene end moraine fans: controls on their sedimentation and location. *Sedimentary Geology*, 149(1–3), 73–92. Available from: https://doi.org/10.1016/S0037-0738(01)00245-7

Larsen, N.K., Piotrowski, J.A., Christoffersen, P. & Menzies, J. (2006) Formation and deformation of basal till during a glacier surge; Elisebreen, Svalbard. *Geomorphology*, 81(1–2), 217–234. Available from: https://doi.org/10.1016/j.geomorph.2006.04.018

Lawson, D.E. (1982) Mobilization, movement and deposition of active subaerial sediment flows, Matanuska Glacier, Alaska. *The Journal of Geology*, 90(3), 279–300. Available from: https://doi.org/10.1086/628680

Le Heron, D.P., Kettler, C., Davies, B.J., Scharfenberg, L., Eder, L., Ketterman, M. et al. (2022) Rapid geomorphological and sedimentological changes at a modern Alpine ice margin: lessons from the Gepatsch Glacier, Tirol, Austria. *Journal of the Geological Society*, 179(3), jgs2021–052. Available from: https://doi.org/10.1144/jgs2021-052

Lee, R.E., Maclachlan, J.C. & Eyles, C.H. (2018) Landsystems of Morsárjökull, Skaftafellsjökull and Svínafellsjökull, outlet glaciers of the Vatnajökull Ice Cap, Iceland. *Boreas*, 47(4), 1199–1217. Available from: https://doi.org/10.1111/bor.12333

Lukas, S. (2005) A test of the englacial thrusting hypothesis of 'hummocky' moraine formation: case studies from the northwest Highlands, Scotland. *Boreas*, 34(3), 287–307. Available from: https://doi.org/10.1111/j.1502-3885.2005.tb01102.x

Lukas, S. (2012) Processes of annual moraine formation at a temperate alpine valley glacier: insights into glacier dynamics and climatic controls. *Boreas*, 41(3), 463–480. Available from: https://doi.org/10.1111/j.1502-3885.2011.00241.x

Lukas, S., Benn, D.I., Boston, C.M., Brook, M., Coray, S., Evans, D.J. et al. (2013) Clast shape analysis and clast transport paths in glacial environments: A critical review of methods and the role of lithology. *Earth-Science Reviews*, 121, 96–116. Available from: https://doi.org/10.1016/j.earscirev.2013.02.005

Magrani, F., Valla, P.G. & Egholm, D. (2021) Modelling alpine glacier geometry and subglacial erosion patterns in response to contrasting climatic forcing. *Earth Surface Processes and Landforms*, 47(4), 1054–1072. Available from: https://doi.org/10.1002/esp.5302

Marren, P.M. & Toomath, S.C. (2013) Fluvial adjustments in response to glacier retreat: Skaftafellsjökull, Iceland. *Boreas*, 42(1), 57–70. Available from: https://doi.org/10.1002/esp.3545

Marren, P.M. & Toomath, S.C. (2014) Channel pattern of proglacial rivers: topographic forcing due to glacier retreat. *Earth Surface Processes and Landforms*, 39(7), 943–951. Available from: https://doi.org/10.1111/j.1502-3885.2012.00275.x

Matthews, J.A., McCarroll, D. & Shakesby, R.A. (1995) Contemporary terminal-moraine ridge formation at a temperate glacier: Styggedalsbreen, Jotunheimen, southern Norway. *Boreas*, 24(20), 129–139. Available from: https://doi.org/10.1111/j.1502-3885.1995.tb00633.x

McCarroll, D. & Rijsdijk, K.F. (2003) Deformation styles as a key for interpreting glacial depositional environments. *Journal of Quaternary Science*, 18(6), 473–489. Available from: https://doi.org/10.1002/jqs.780

Oerlemans, J. (2012) Linear modelling of glacier length fluctuations. *Geografiska Annaler. Series a, Physical Geography*, 94(2), 183–194. Available from: https://doi.org/10.1111/j.1468-0459.2012.00469.x

Paul, F. & Andreassen, L.M. (2009) A new glacier inventory for the Svartisen region, Norway, from Landsat ETM+ data: challenges and change assessment. *Journal of Glaciology*, 55(192), 607–618. Available from: https://doi.org/10.3189/002214309789471003

Pedersen, V.K. & Egholm, D.L. (2013) Glaciations in response to climate variations preconditioned by evolving topography. *Nature*, 493(7431), 206–210. Available from: https://doi.org/10.1038/nature11786

Phillips, E., Merritt, J., Auton, C. & Golledge, N. (2007) Microstructures in subglacial and proglacial sediments: understanding faults, folds and fabrics, and the influence of water on the style of deformation. *Quaternary Science Reviews*, 26(11–12), 1499–1528. Available from: https://doi.org/10.1016/j.quascirev.2007.03.007

Price, R.J. (1970) Moraines at Fjallsjökull, Iceland. *Arctic and Alpine Research*, 2(1), 27–42. Available from: https://doi.org/10.1080/00040851.1970.12003559

Rabot, C. (1898) *Au Cap Nord: itinéraires en. Norvège, Suède el Finlande*. Paris, Hachette.

Reinardy, B.T., Booth, A.D., Hughes, A.L., Boston, C.M., Åkesson, H., Bakke, J. et al. (2019) Pervasive cold ice within a temperate glacier– implications for glacier thermal regimes, sediment transport and foreland geomorphology. *The Cryosphere*, 13(3), 827–843. Available from: https://doi.org/10.5194/tc-13-827-2019

Reinardy, B.T., Leighton, I. & Marx, P.J. (2013) Glacier thermal regime linked to processes of annual moraine formation at Midtdalsbreen, southern Norway. *Boreas*, 42(4), 896–911. Available from: https://doi.org/10.1111/bor.12008

Rekstad, J. (1893) Beretning om en undersøgelse af Svartisen, foretagen i somrene 1890 og 1891. *Archiv for Mathematik og Naturvidenskab*, 16, 266–231.

Rounce, D.R., Hock, R., Maussion, F., Hugonnet, R., Kochtitzky, W., Huss, M. et al. (2023) Global glacier change in the 21st century: every increase in temperature matters. *Science*, 379(6627), 78–83. Available from: https://doi.org/10.1126/science.abo1324

Rowan, A.V., Egholm, D.L. & Clark, C.D. (2022) Forward modelling of the completeness and preservation of palaeoclimate signals recorded by ice-marginal moraines. *Earth Surface Processes and Landforms*, 47(9), 2198–2208. Available from: https://doi.org/10.1002/esp.5371

Schomacker, A. (2010) Expansion of ice-marginal lakes at the Vatnajökull ice cap, Iceland, from 1999 to 2009. *Geomorphology*, 119(3–4), 232–236. Available from: https://doi.org/10.1016/j.geomorph.2010.03.022

Sharov, A. (2003) Gradient approach to INSAR modelling of glacial dynamics and morphology. In: *Proc. 22d EARSeL Symp*. Rotterdam, Millpress, pp. 373–381. Available from: http://www.earsel.org/symposia/2002-symposium-Prague/pdf/051.pdf

Sharp, M. (1984) Annual moraine ridges at Skálafellsjökull, south-east Iceland. *Journal of Glaciology*, 30(104), 82–93. Available from: https://doi.org/10.3189/S0022143000008522

Staines, K.E., Carrivick, J.L., Tweed, F.S., Evans, A.J., Russell, A.J., Jóhannesson, T. et al. (2015) A multi-dimensional analysis of proglacial landscape change at Sólheimajökull, southern Iceland. *Earth Surface Processes and Landforms*, 40(6), 809–822. Available from: https://doi.org/10.1002/esp.3662

Stokes, C.R., Andreassen, L.M., Champion, M.R. & Corner, G.D. (2018) Widespread and accelerating glacier retreat on the Lyngen Peninsula, northern Norway, since their 'Little Ice Age' maximum. *Journal of Glaciology*, 64(243), 100–118. Available from: https://doi.org/10.1017/jog.2018.3

Theakstone, W.H. (2010) Glacier changes at Svartisen, Northern Norway, during the last 125 years: influence of climate and other factors. *Journal of Earth Science*, 21(2), 123–136. Available from: https://doi.org/10.1007/s12583-010-0011-6

Thome, K.N. (1972) Asymmetries in glacier structure and their influence on glacier movement and glacier deposition. In: *Proceedings of the 24th international geological congress (Canada)*. Section 12, pp. 198–211.

UNESCO & IUCN. (2022) *World heritage glaciers: sentinels of climate change, Paris*. UNESCO; Gland, IUCN. Available from: https://unesdoc.unesco.org/ark:/48223/pf0000383551

Weber, P., Andreassen, L.M., Boston, C.M., Lovell, H. & Kvarteig, S. (2020) An ∼1899 glacier inventory for Nordland, northern Norway, produced from historical maps. *Journal of Glaciology*, 66(256), 259–277. Available from: https://doi.org/10.1017/jog.2020.3

Weber, P., Boston, C.M., Lovell, H. & Andreassen, L.M. (2019) Evolution of the Norwegian plateau icefield Hardangerjøkulen since the 'Little Ice Age'. *The Holocene*, 29(12), 1885–1905. Available from: https://doi.org/10.1177/0959683619865601

Winkler, S. (2003) A new interpretation of the date of the 'Little Ice Age' glacier maximum at Svartisen and Okstindan, northern Norway. *The Holocene*, 13(1), 83–95. Available from: https://doi.org/10.1191/0959683603hl573rp

Winkler, S. (2021) Terminal moraine formation processes and geomorphology of glacier forelands at the selected outlet glaciers of Jostedalsbreen, South Norway. In: Beylich, A.A. (Ed.) *Landscapes and landforms of Norway*. Cham: Springer, pp. 33–69 https://doi.org/10.1007/978-3-030-52563-7_3

Winkler, S. & Matthews, J.A. (2010) Observations on terminal moraine-ridge formation during recent advances of southern Norwegian glaciers. *Geomorphology*, 116(1–2), 87–106. Available from: https://doi.org/10.1016/j.geomorph.2009.10.011

Worsley, P. (1974) Recent "annual" moraine ridges at Austre Okstindbreen, Okstindan, North Norway. *Journal of Glaciology*, 13(68), 265–277. Available from: https://doi.org/10.3189/S0022143000023078

Wyshnytzky, C.E., Lukas, S. & Groves, J.W. (2020) Multiple mechanisms of minor moraine formation in the Schwarzensteinkees Foreland, Austria. In: Waitt, R.B., Thackray, G.D. & Gillespie, A.R. (Eds.) *Untangling the quaternary period—a legacy of Stephen C. Porter*, Geological Society of America Special Paper, Vol. 548, pp. 193–207. https://doi.org/10.1130/2020.2548(10)

Zemp, M., Frey, H., Gärtner-Roer, I., Nussbaumer, S.U., Hoelzle, M., Paul, F. et al. (2015) Historically unprecedented global glacier decline in the early 21st century. *Journal of Glaciology*, 61(228), 745–762. Available from: https://doi.org/10.3189/2015JoG15J017

Zemp, M., Huss, M., Thibert, E., Eckert, N., McNabb, R., Huber, J. et al. (2019) Global glacier mass changes and their contributions to sea-level rise from 1961 to 2016. *Nature*, 568(7752), 382–389. Available from: https://doi.org/10.1038/s41586-019-1071-0